HOSTED BY

ELSEVIER

Contents lists available at ScienceDirect

Geoscience Frontiers

journal homepage: www.elsevier.com/locate/gsf



Research Paper

Early Mesoproterozoic evolution of midcontinental Laurentia: Defining the geon 14 Baraboo orogeny



L. Gordon Medaris Jr ^{a,*}, Brad S. Singer ^a, Brian R. Jicha ^a, David H. Malone ^b, Joshua J. Schwartz ^c, Esther K. Stewart ^d, Amanda Van Lankvelt ^e, Michael L. Williams ^f, Peter W. Reiners ^g

- ^a Department of Geoscience, University of Wisconsin–Madison, Madison, WI 53706, USA
- ^b Department of Geography, Geology & Environment, Illinois State University, Normal, IL 61790, USA
- ^c Department of Geological Sciences, California State University-Northridge, Northridge, CA 91330, USA
- ^d Wisconsin Geological & Natural History Survey, Madison, WI 53705, USA
- ^e Cameca Instruments, 5470 Nobel Dr., Madison, WI 54711, USA
- f Department of Geosciences, University of Massachusetts-Amherst, Amherst, MA 01003, USA
- g Department of Geosciences, University of Arizona, Tucson, AZ 85721, USA

ARTICLE INFO

Article history: Received 12 November 2020 Received in revised form 4 February 2021 Accepted 7 February 2021 Available online 20 February 2021

Handling Editor: C. J. Spencer

Keywords:
Mesoproterozoic orogeny
Ferroan granite
Detrital zircon

40Ar/39Ar geochronology
U-Th-total Pb geochronology
U/Th-He geochronology

ABSTRACT

New geochronologic data from midcontinental Laurentia demonstrate that emplacement of the 1476-1470 Ma Wolf River granitic batholith was not an isolated igneous event, but was accompanied by regional metamorphism, deformation, and sedimentation. Evidence for such metamorphism and deformation is best seen in siliciclastic sedimentary rocks of the Baraboo Interval, which were deposited closely following the 1.65-1.63 Ga Mazatzal orogeny. In Baraboo Interval strata, muscovite parallel to slatey cleavage, in hydrothermal veins, in quartzite breccia, and in metamorphosed paleosol yielded ⁴⁰Ar/³⁹Ar plateau ages of 1493–1465 Ma. In addition, U-Th-total Pb dating of neoblastic overgrowths on detrital monazite gave an age of 1488 ± 20 Ma, and recrystallized hematite in folded metapelite gave a mean U/Th-He age of 1411 ± 39 Ma. Post-Baraboo, arkosic polymictic conglomerate, which contains detrital zircon with a minimum peak age of 1493 Ma, was intruded by a 1470 Ma granite porphyry at the northeastern margin of the Wolf River batholith. This episode of magmatism, regional deformation and metamorphism, and sedimentation, which is designated herein as the Baraboo orogeny, provides a midcontinental link between the Picuris orogeny to the southwest and the Pinware orogeny to the northeast, completing the extent of early Mesoproterozoic (Calymmian) orogenesis for 5000 km along the southern margin of Laurentia. This transcontinental orogen is unique among Precambrian orogenies for its great width (~1600 km), the predominance of ferroan granites derived from partial melting of lower continental crust, and the prevalence of regional high T-P metamorphism related to advective heating by granitic magmas emplaced in the middle to upper crust.

© 2021 China University of Geosciences (Beijing) and Peking University. Production and hosting by Elsevier B.V. This is an open access article under the CC BY-NC-ND license (http://creativecommons.org/licenses/by-nc-nd/4.0/).

1. Introduction

The 1476–1470 Ma Wolf River batholith is a prominent and important feature in the Precambrian geology of Wisconsin, being the local member of a transcontinental suite of geon 14 granites (Anderson, 1983), where the term, geon, refers to a 100 Ma interval of time (Hofman, 1990). The batholith was first identified by Van Schmus et al. (1975a), when it was interpreted to be an anorogenic feature, based on the prevailing petrologic and tectonic paradigms for the southern Lake Superior region (SLSR) at that time. However, we now document here that emplacement of the Wolf River batholith was accompanied by regional deformation, metamorphism, and sedimentation. Thus, the

* Corresponding author. E-mail address: medaris@geology.wisc.edu (L.G. Medaris). batholith was not an isolated igneous phenomenon, but rather, represents the igneous component of a distinctive geon 14 tectonomagmatic event in the Laurentian midcontinent.

In this investigation, new detrital zircon ages constrain the ages for two episodes of early Mesoproterozoic (Calymmian) sedimentation in the SLSR, the earlier episode being deposition of the Baraboo Interval quartzites after ~1.63 Ga (post–Mazatzal), and the later one being deposition of the Baldwin conglomerate after ~1.46 Ga. In Baraboo Interval quartzites, new U–Th–total Pb ages for metamorphic monazite (1488 \pm 20 Ma) and U/Th–He ages for metamorphic hematite (1411 \pm 39 Ma), combined with previously published and recalculated $^{40}\text{Ar}/^{39}\text{Ar}$ ages for metamorphic muscovite (1493–1465 Ma), document the timing and effects of deformation, metamorphism, and K–metasomatism over a broad area in the SLSR. Consequently, we propose that this geon 14 tectonomagmatic event formally be called the

"Baraboo orogeny", which provides a midcontinental link between the Picuris orogeny to the southwest and the Pinware orogeny to the northeast, thus completing the transcontinental extent of geon 14 orogenesis for 5000 km along the southern margin of Laurentia.

2. Precambian framework of the Southern Lake Superior region

The Precambrian history of the SLSR is a 2.5-billion-year saga that begins at 3.5 Ga with Paleoarchean growth of the Superior Craton to the north and west and ends at 1.1 Ga with Mesoproterozoic magmatism and sedimentation associated with rifting of midcontinental North America (Figure 1). The interim was occupied consecutively by:

- 2.45–1.77 Ga deposition of craton margin and foreland basin sediments on the Archean craton, a 1.89–1.83 Ga growth and accretion of volcanic arc associations in the Penokean Province;
- 1.80–1.75 Ga emplacement of granites in the Penokean Province in east–central Minnesota and northern Wisconsin and granites and rhyolites in the Yavapai Province in southern Wisconsin;
- ~1.63 Ma recrystallization of Penokean and Yavapai basement in Wisconsin (note the 1.63 Ga thermal front in Fig. 1);
- post–Mazatzal (≤1.63 Ga) deposition of Baraboo Interval quartzites;
- 1.47 Ga emplacement of the Wolf River batholith.

2.1. Archean superior province

The Archean Superior Province in the SLSR is divided by the late Neoarchean Great Lakes tectonic zone (GLTZ) into the Wawa Subprovince to the north and the Minnesota River Valley Subprovince to the south (Fig. 1; Holm et al., 2007a). The 2750–2680 Ma Wawa

Subprovince is a classic granite–greenstone belt, comprising accreted island arcs consisting of nearly vertical belts of metavolcanic and metasedimentary rocks and associated elongate granitoid batholiths (Williams, 1990). In contrast, the Minnesota River Valley Subprovince is dominated by migmatitic gneisses with 3500–3400 Ma protolith ages that were intruded by ca. 2600 Ma granitic plutons, all of which were accreted to the southern margin of the Superior Province at ca. 2600 Ma during the Algoman orogeny (Bickford et al., 2006; Schmitz et al., 2006; Satkowski et al., 2013).

2.2. Craton Margin Domain and Penokean Province

Sedimentary rocks of the Craton Margin Domain (Fig. 1) include siliciclastic sediments, carbonate, and glaciogenic strata that were deposited between 2.45 and 2.2 Ga in rift basins developed on the Archean continental margin. Following a 300 Ma hiatus, these rift-related strata were succeeded by predominantly arc–derived turbidites that were deposited between 1.89 and 1.77 Ga in the foreland basin of the Penokean arc (Young, 1983; Ojakangas et al., 2001a; Schulz and Cannon, 2007). Included in this latter sedimentary section are the geologically and economically important iron-formations of the region that were deposited between 1.88 and 1.86 Ga (Schneider et al., 2002).

In the Penokean Province, the Wausau–Pembine terrane developed as an oceanic volcanic arc at ~1890 Ma that was subsequently accreted to the margin of the Superior craton at ~1875 Ma (Fig. 1; Schulz and Cannon, 2007). The Marshfield terrane originated south (present day coordinates) of the Wausau–Pembine terrane and comprises an island arc built on an exotic fragment of Archean crust (Van Schmus and Anderson, 1977); this composite terrane was then accreted to the Wausau–Pembine terrane at ~1850 Ma, at which time the Penokean

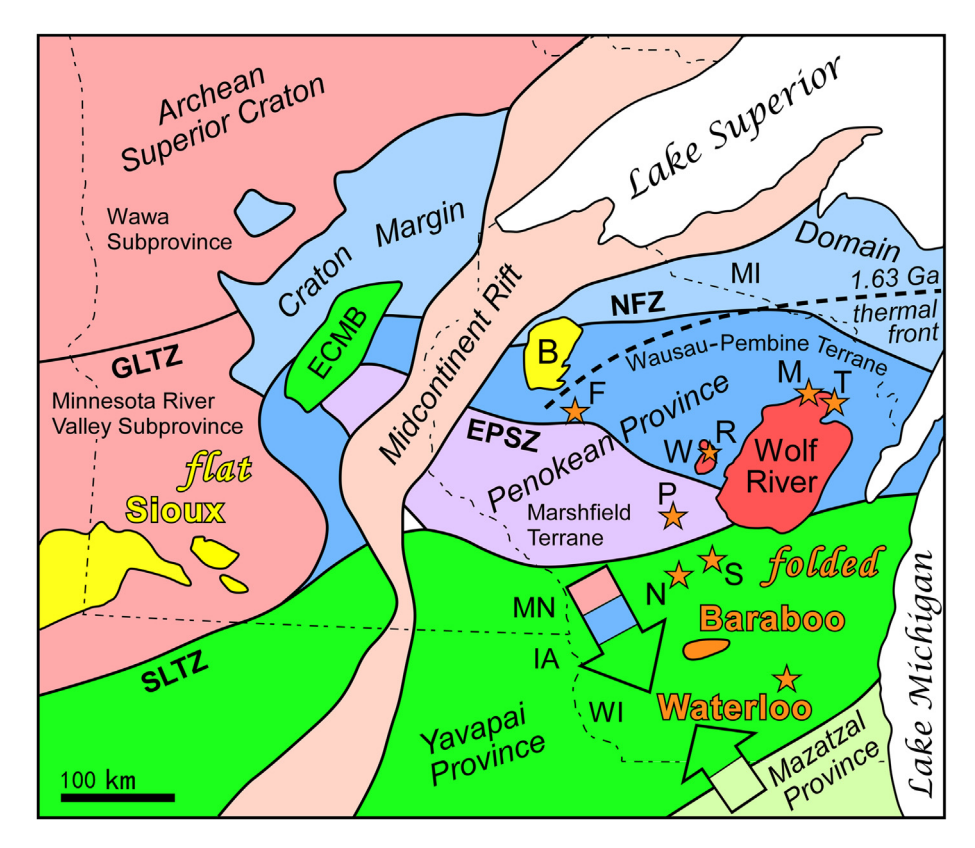


Fig. 1. Geological map of Precambrian terranes and the Wolf River batholith in the southern Lake Superior region (modified from Romano et al., 2000; Holm et al., 2007a; Holm et al., 2007b; Whitmeyer and Karlstrom, 2007). Baraboo Interval quartzites to the northwest (in yellow) are flat-lying, and those to the southeast (in orange) are folded. Quartzite abbreviations: B, Barron; F, Flambeau; M, McCaslin; N, Necedah; P, Powers Bluff (including Veedum and Vesper); R, Rib Mountain; S, Seven Sisters; T, Thunder Mountain. Arrows illustrate generalized sediment transport directions for Baraboo Interval quartzites, with provenances indicated by colors. Other abbreviations: ECMB, East Central Minnesota Batholith; EPSZ, Eau Pleine shear zone; GLTZ, Great Lakes tectonic zone; NFZ, Niagara fault zone; SLTZ, Spirit Lake tectonic zone; W, Wausau syenite–granite complex (in red).

foreland basin was initiated. Plutonic and volcanic arc associations in both terranes are calc-alkalic and magnesian in composition, and magmatic activity continued until ~1.83 Ga, when stitching plutons were emplaced across the amalgamated terranes (Anderson and Cullers, 1987; Sims et al., 1989; Schulz and Cannon, 2007).

2.3. Yavapai Province

The geon 17 Yavapai Province in the SLSR is largely covered by Paleozoic cratonic strata, although basement inliers are scattered widely across this region, and the distribution of such inliers, combined with drill core samples of basement, reveal the widespread extent of the Yavapai Province along the southern margin of Laurentia (Fig. 1). The Yavapai basement in Wisconsin consists of calc-alkalic rhyolites and granites of the 1750 Ma Montello Batholith, including both metaluminous and peraluminous types (Smith, 1978, 1983; Anderson et al., 1980; Holm et al., 2005; Van Schmus et al., 2007). This magmatic suite in southern Wisconsin, which underlies a minimum area of 6500 km², is K-feldspar rich and ferroan in composition, in contrast to Penokean granitoids, which are plagioclase-rich and magnesian. Additional geon 17 plutons in the region, outside the Yavapai Province itself, include the 1787-1772 Ma East Central Minnesota Batholith (Fig. 1), which is located west of the Midcontinent Rift where it intrudes the Craton Margin Domain and Penokean Province, and three other small plutons in northern Wisconsin (not shown in Fig. 1), viz. the 1781 Ma Park Falls granite north of the Niagara Fault Zone, the 1776 Ma Radisson granite south of the fault zone in the Wausau-Pembine terrane, and a 1760 Ma granite in the Marshfield terrane (Holm et al., 2005; Craddock et al., 2018). The northwest to southeast decrease in age from the 1787-1772 Ma East Central Minnesota Batholith to the 1750 Ma Montello Batholith has been attributed to slab rollback during geon 17 subduction of oceanic crust beneath the Laurentian margin (Holm et al., 2005). Geon 17 arc development was accompanied by extensive amphibolite facies metamorphism and deformation in the geon 18 Penokean Province (Holm et al., 2020).

2.4. Mazatzal Province

The geon 16 Mazatzal Province lies south of the Yavapai Province along the southern margin of the SLSR (Fig. 1), where it is buried by Paleozoic strata. The hidden Mazatzal terrane in the SLSR is thought to be an island arc that was accreted to Laurentia at 1650-1630 Ma (Holm et al., 2007b). The presence of Mazatzal crust beneath the Illinois Basin is inferred from the occurrence of geon 16 detrital zircon grains in basal Cambrian strata from deep drill core, in which 14 of 100 detrital zircon grains range in age from 1628 to 1683 Ma with a mean age of 1658 \pm 14 Ma (Freiburg et al., 2020). Although Mazatzal crust itself is unknown in Wisconsin, the effects of geon 16 metamorphism are widespread in the Penokean and Yavapai Provinces there. A 1.63 Ga thermal front has been identified in northern Wisconsin and the Upper Peninsula of Michigan (Fig. 1; Holm et al., 1998; Romano et al., 2000; Holm et al., 2007b), south of which mica in the Penokean and Yavapai provinces has 40Ar/39Ar cooling ages of 1614-1576 Ma, and amphibole has a range of ages from 1796 Ma to 1638 Ma, due to partial resetting at ~1650-1630 Ma. The effects of such recrystallization are also evident in the Montello batholith in southern Wisconsin, which has a 1750 Ma crystallization age and a 1650 Ma Rb-Sr whole-rock isochron age (Van Schmus et al., 1975b). In addition, although 1750 Ma diorite, granite, and rhyolite in the Baraboo Range in south-central Wisconsin retain their igneous textures and structures, they have been pervasively recrystallized under greenschist facies conditions, with calcic plagioclase having been replaced by albite + epidote, biotite by chlorite, and hornblende by chlorite + actinolite (Medaris Jr., 2001 and Dott Jr., 2001).

2.5. Baraboo Interval sedimentary rocks

The term, Baraboo Interval, was introduced to encompass the deposition of red, supermature quartzites in the SLSR between ~1750 Ma, the age of the youngest underlying basement, and ~ 1475 Ma, the age of intrusive Wolf River granites. These quartzites are key to interpreting the Mesoproterozoic (Calymmian) evolution of the SLSR, including the timing of sedimentation, the physiographic and climatic conditions at the time of deposition, and the chronology of folding and associated metamorphism. Baraboo Interval siliciclastic sediments were deposited over a minimum area of ~300,000 km² in the midcontinent (; Ojakangas and Weber, 1984; Southwick et al., 1986; Medaris Jr. et al., 2003), where they are nonconformable on Archean, Penokean, and Yavapai basement (Fig. 1). Individual sedimentary sections across the region progress upward from fluvial facies to shoreface marine facies and consist predominantly of quartz arenite, accompanied by subordinate amounts of quartz pebble conglomerate, quartz siltstone, and kaolinite mudstone.

Baraboo Interval sediments were originally interpreted to have been deposited as a southward-thickening clastic wedge on the southern margin of Laurentia, although subsidence modelling calls for local extension or transtension to provide the accommodation space necessary for deposition of some quartzite sequences up to 1500 m thick (Stewart et al., 2018). Baraboo Interval quartzites are flat lying in the north and west of the region and folded and metamorphosed in the south and east (Fig. 1), where the separate quartzite localities represent synclinal domains that remain after folding and subsequent erosion.

2.6. Wolf River Batholith

The 1476–1470 Ma Wolf River batholith is a ferroan rapakivi granite massif that underlies an area of ~9200 km² in east-central Wisconsin, where it intrudes the Penokean Province (both the Wausau-Pembine and Marshfield terranes), the Yavapai Province, and Baraboo Interval quartzites (Fig. 1; Van Schmus et al., 1975a; Anderson and Cullers, 1978; Anderson, 1980; DeWayne and Van Schmus, 2007;). The Wolf River batholith is the only geon 14 igneous unit exposed in the SLSR, although granites of this age are distributed widely in the subsurface to the south (Bickford et al., 2015). Other post-Baraboo Interval granitic rocks in the region occur in the Wausau syenite-granite complex, which is located ~15 km west of the Wolf River batholith (Fig. 1; Myers et al., 1984; Medaris Jr. and Koellner, 2010). This complex consists of four overlapping, concentric, epizonal plutons, three of which have U-Pb zircon ages of 1565 \pm 4 Ma, 1522 \pm 6 Ma, and 1506 \pm 3 Ma (Van Wyck et al., 1994; DeWayne and Van Schmus, 2007). Although the Wausau complex is 30-90 Ma older than the Wolf River batholith, it shares many petrologic characteristics, such as a ferroan composition. The Wausau complex was emplaced following Baraboo Interval sedimentation, thus suggesting that it may represent a precursor to the Wolf River batholith and other geon 14 transcontinental ferroan granites.

2.7. Midcontinent Rift

The final episode in the Precambrian evolution of the SLSR was development of the ~1100 Ma Midcontinent Rift System (Fig. 1), which extends for ~1800 km from Lake Superior to Oklahoma (Hinze et al., 1997; Ojakangas et al., 2001b). The rift is made up of a series of axial halfgrabens, separated by accommodation zones, that are filled with ~20 km of volcanic rocks and ~10 km of overlying sedimentary rocks. The 1109–1087 Ma volcanic rocks, which consist of ~90% tholeiitic flood basalt and ~10% rhyolite and icelandite, are accompanied by a variety of intrusive rocks, including alkalic plutons, layered tholeiitic intrusions, and quartz and olivine tholeiite dikes and sills (Weiblen, 1982). The post–rift clastic sedimentary rocks include two groups: an early, immature, alluvial fan to fluvial red bed sequence with an intra–basin provenance, and a later, more mature, fluvial red bed sequence with

an extra-basin provenance (Ojakangas et al., 2001b). The original normal faults of the rift were reactivated and inverted to high-angle reverse faults, accompanied by development of an uplifted central horst. Previously, such structural features were interpreted as reflecting far-field effects of the Grenville orogeny to the east, but more recent work has demonstrated that basin inversion was a post-Grenville, Paleozoic reactivation phenomenon (Malone et al., 2016; Craddock et al., 2017).

3. Analytical methods

3.1. ⁴⁰Ar/³⁹Ar dating of muscovite (University of Wisconsin–Madison)

Previously, 40 Ar/ 39 Ar plateau ages for single muscovite crystals were determined by step heating, using a defocused CO_2 laser in the WiscAr Lab at the Department of Geoscience, UW–Madison, following the methods described in Medaris Jr et al. (2002, 2009); Medaris Jr. et al. (2003) and Medaris Jr. and Singer (2010). In this investigation, the 40 Ar/ 39 Ar ages for the previously analyzed samples have been recalculated relative to the 28.201 Ma Fish Canyon sanidine standard (Kuiper et al., 2008), which supersedes the prior standard, using the decay constants of Min et al. (2000). The complete analytical data are given in Supplementary data, Table 4.

3.2. LA-ICPMS U-Pb zircon geochronology (Arizona LaserChron Center)

Zircon from two samples of Waterloo quartzite, which is the southeasternmost of the Baraboo Interval occurrences, and one of Baldwin conglomerate was separated by conventional gravitational and magnetic techniques. U-Pb geochronology of zircon was conducted by laser ablation-inductively coupled plasma mass spectrometry (LA-ICPMS) at the Arizona LaserChron Center, following the methods of Gehrels et al. (2006, 2008) and Gehrels and Pecha (2014). Unknown zircons were mounted with the standard Sri Lanka, FC-1, and R33 zircons on a 1" puck with epoxy, sanded down to a depth of ~20 µm, polished, and cleaned prior to analysis. The analyses were performed by ablation of zircon with a Photon Machines Analyte G2 excimer laser equipped with HelEx ablation cell using a spot diameter of 20 µm. The ablated material was carried in helium into the plasma source of an Element2 HR ICPMS. Following analysis, data reduction was performed with an in-house Python decoding routine and an Excel spreadsheet (E2agecalc) that determined a "best age" for each analysis, which is generally the 206/238 age for ages <900 Ma and the 206/207 age for ages > 900 Ma, and rejected analyses with > 10% discordance, >5% reverse discordance, >400 ppm Pb²⁰⁴ or >10% internal (measurement) uncertainty. The ages are presented on relative ageprobability diagrams using routines in Isoplot (Ludwig, 2012).

3.3. LA-SF-ICPMS U–Pb zircon geochronology (California State University, Northridge)

Zircon was separated from five samples of Waterloo quartzite following standard methods involving crushing, pulverizing with jaw crusher and disk mill, and density separation on a Wilfley gold table and with heavy liquids. Samples were processed through a Frantz isodynamic separator (side tilt = 5° , front tilt = 20°) at 0.5 amps to remove magnetic (non-zircon) minerals. Zircon was poured onto double sided tape and mounted in epoxy, ground and polished, followed by imaging on a Gatan MiniCL detector attached to a FEI Quanta 600 SEM at California State University Northridge.

Uranium-lead ratios were collected using a ThermoScientific Element2 SF-ICPMS coupled with a Teledyne Cetec Analyte G2 Excimer Laser (operating at a wavelength of 193 nm). Prior to analysis, the Element2 instrument was tuned using the NIST 612 glass standard to optimize signal intensity and stability. Laser beam diameter was ~30–40 µm at 10 Hz and 75%–100% power. Ablation was performed in a HelEx II Active 2-Volume Cell™ and sample aerosol was transported with He

carrier gas through Teflon-lined tubing, where it was mixed with Ar gas before introduction to the plasma torch. Flow rates for Ar and He gases were as follows: Ar cooling gas (16.0 NL/min), Ar auxiliary gas (1.0 NL/min), He carrier gas (~0.3–0.5 NL/min), Ar sample gas (1.1–1.3 NL/min). Isotope data were collected in *E*-scan mode with magnet set at mass 202, and RF Power at 1245 W. Isotopes measured include 202 Hg, 204 (Pb + Hg), 206 Pb, 207 Pb, 208 Pb, 232 Th, and 238 U. All isotopes were collected in counting mode except for 232 Th and 238 U, which were collected in analogue mode. Analyses were conducted in a ~ 40-min time resolved analysis mode. Each zircon analysis consisted of a 20-s integration with the laser firing on sample, and a 20 s delay to purge the previous sample and move to the next sample. Approximate depth of the ablation pit was ~20–30 μ m.

The primary standard, 91,500, was analyzed every 5–10 analyses to correct for in-run fractionation of Pb/U and Pb isotopes. The second zircon standards, R33 and Plesovice, were analyzed every ~10 analyses to assess reproducibility of the data. Total uncertainties (analytical \pm systematic) were determined by lolite (Paton et al., 2011). U–Pb analysis of R33 and Plesovice during all analytical sessions yielded concordant results and error-weighted average ages of 423.5 \pm 3.3 Ma (n=39) and 337.6 \pm 4.4 Ma (n=48), both of which are within close agreement of the accepted ages for R33 (419 Ma: Black et al., 2004), and Plesovice (337 Ma: Sláma et al., 2008).

U–Pb isotopic data were plotted using Isoplot 4.15 (Ludwig, 2012). Corrections for minor amounts of common Pb in zircon were made following the methods of Tera and Wasserburg (1972), using measured 207 Pb/ 206 Pb and 238 U/ 206 Pb ratios and an age appropriate Pb isotopic composition of Stacey and Kramers (1975). Zircon analyses with large common Pb corrections (e.g., analyses interpreted as having ~5% or greater contribution from common Pb) were discarded from further consideration. Zircon dates are reported using the 206 Pb/ 238 U date for zircon <1400 Ma, and the 207 Pb/ 206 Pb date for zircon >1400 Ma.

A 10% discordance filter was applied to all data. For zircon >1400 Ma, discordance is calculated as the percent difference between the $^{207}\text{Pb}/^{206}\text{Pb}$ date and $^{206}\text{Pb}/^{238}\text{U}$ date. For zircon younger than 1400 Ma, the $^{207}\text{Pb}/^{206}\text{Pb}$ date is an unreliable indicator of discordance due to low abundances of measured ^{207}Pb . For such zircon, discordance is calculated as the percent difference between the $^{207}\text{Pb}/^{235}\text{U}$ date and $^{206}\text{Pb}/^{238}\text{U}$ date.

3.4. (U–Th)/He dating of hematite (University of Arizona)

We measured (U-Th)/He ages of multiple aliquots of hematite as single crystals or agglomerates of several crystallites. Detailed methods are described in Evenson et al. (2014), but a brief description follows. Hematite-bearing fragments were selected from hand-crushed wholerock samples and treated ultrasonically to isolate hematite crystals or crystal aggregates with minimal proportions of other phases (largely quartz in this case). Aliquots with dimensions on the order of tens of mm were characterized by photomicroscopy and loaded into 1-mm Nb tubes, heated to $\sim 900-1200$ °C by diode laser in $<\sim 10^{-8}$ Torr chamber. Released gases were spiked with ³He, He was cryogenically purified, and ⁴He was quantified by sample-standard bracketing on spiked aliquots of calibrated ⁴He standard shots. Uranium and Th were measured by isotope dilution on the same aliquots using HR-ICP-MS, following spiking and bomb-acid dissolution. Concentrations of U and Th were measured using mass determinations based on both microbalance and standard-peak comparisons on Fe measurements by ICP-MS and assuming stoichiometric Fe₂O₃, which agreed to ~10 to 15%. Aliquots of hematite from samples other than 17BQ15 (not reported here) had low eU (U + 0.24*Th) of 1–2 ppm, resulting in relatively large uncertainties, and aliquots for many of those (non-17BQ15) samples showed evidence for large U-losses (e.g., Hofmann et al., 2020) during lasing for He extraction, compared with unlased aliquots of the same samples. Here we only report results from aliquots from sample 17BQ15 that did not display this behavior, showed no systematic difference between age/composition ratios between low and intense lasing conditions, and had eU > 4 ppm.

3.5. U-Th-total Pb dating of monazite (University of Massachusetts–Amherst)

Monazite dating was carried out at the University of Massachusetts using the methods of Williams et al. (2017). In brief, the ca. 20 µm-wide monazite grains were located using full-thin-section compositional mapping. For this study, maps were collected for Mg, K, Ca, Ce, and Zr. The Mg, K, and Ca maps show the distribution of the major silicate phases, and the Ce and Zr maps show the location of monazite and zircon grains, respectively. Individual monazite grains were mapped at high resolution ($<0.5 \,\mu$ step size) for Y, Th, U, Ca, and one other element (Si, Nd, Gd, As, etc.). The maps were processed simultaneously such that intensities were comparable from grain map to grain map. Monazite dating was carried out on the Cameca Ultrachron electron microprobe at the University of Massachusetts. For each compositional domain, a single background analysis was acquired first, followed by 4-8 peak measurements near the background location. Background intensities were determined using the "multipoint" method (Allaz et al., 2019), and one "date" was calculated for each domain. Uncertainty was calculated by propagating measurement and background errors through the age equation (Williams et al., 2006). Dates are shown as a single Gaussian probability distribution function (curve) for the dated domain.

4. Baraboo interval quartzites: Depositional age and composition

The depositional age, mineral and chemical compositions, and structural features of Baraboo Interval sedimentary rocks are essential for deciphering the Mesoproterozoic (Calymmian) evolution of the SLSR. Baraboo Interval quartzites were deposited between 1643 \pm 11 Ma, the Maximum Depositional Age (MDA) for detrital zircon in quartzite, as described below, and 1506 \pm 2.7 Ma, the age of granite that intrudes quartzite in the Wausau complex (DeWayne and Van Schmus, 2007).

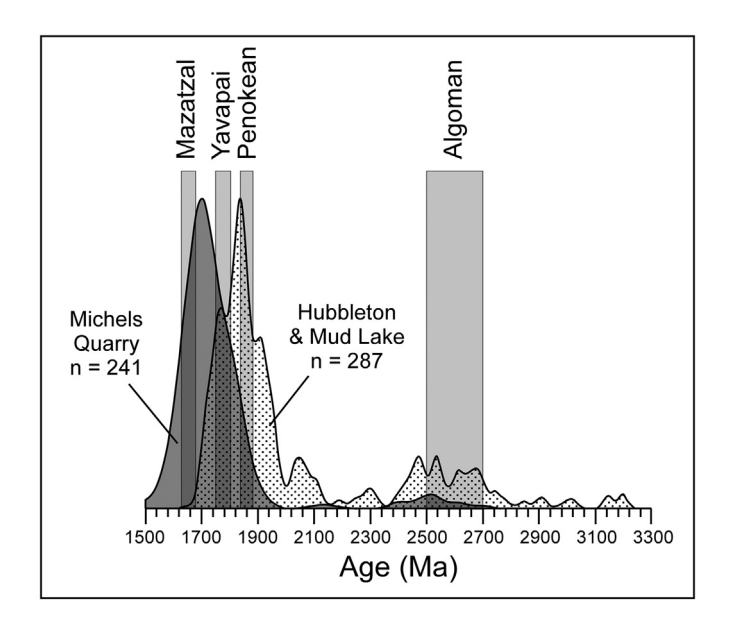


Fig. 2. Composite relative probability plot for detrital zircon in quartzite from the Michels Quarry in the lower part of the Waterloo quartzite. Also shown is a composite relative probability plot for detrital zircon from two samples of quartzite higher in the Waterloo section at the Hubbleton and Mud Lake localities. The age spans of orogenies in the southern Lake Superior region are indicated by the vertical bars.

The transport direction for clastic detritus in most Baraboo Interval localities was generally from northwest to southeast, as determined by paleocurrent measurements (Dalziel and Dott Jr., 1970), which are indicated by the tricolored arrow in Fig. 1, and detrital zircon consequently exhibits Yavapai, Penokean, and Algoman ages of the underlying basement (Van Wyck, 1995; Holm et al., 1998; Medaris Jr. et al., 2003; Van Wyck and Norman, 2004 Stewart et al., 2018;). In the Baraboo Range in southcentral Wisconsin (Fig. 1), detrital zircon age populations in the lower fluvial facies of the quartzite differ from those in the upper shoreface marine facies (Van Wyck and Norman, 2004; Schwartz et al., 2018; Stewart et al., 2018). Detrital zircon in the lower quartzites displays a predominant geon 17 peak, reflecting derivation largely from the underlying, proximal 1750 Ma Montello batholith; subsequent deposition buried the geon 17 basement, and age populations of detrital zircon in the upper quartzites shift to those of more distal geon 18 Penokean and geon 25 Algoman provenances.

Scattered outcrops of supermature quartzite in southeastern Wisconsin, which are referred to collectively as the Waterloo quartzite (Fig. 1), provide the definitive constraint on the maximum depositional age of the Baraboo Interval. Although paleocurrent directions have not been measured in the Waterloo quartzite, the presence of geon 16 detrital zircon grains in the lower part of the quartzite sequence (at the Michels quarry) indicates a southern, Mazatzal provenance, as illustrated by the bicolored arrow in Fig. 1. Quartzite from the Michels quarry displays a prominent combined geon 16 (Mazatzal) and geon 17 (Yavapai) signal, and diminished geon 18 (Penokean) and geon 25-27 (Algoman) signals (Fig. 2; Supplementary data, Table 2). An abundance of geon 16 detrital zircon grains in five samples of quartzite from the Michels quarry and a maximum depositional age of 1643 \pm 11 Ma (n = 42; MSWD = 1.05) for quartzite sample 17WQ-8 demonstrate that deposition of the Waterloo Quartzite was a late- or post-Mazatzal event and imply that correlative Baraboo Interval quartzites in the region also represent late- or post-Mazatzal deposition. Stratigraphically higher in the Waterloo quartzite at the Hubbleton and Mud Lake localities, sediment provenance shifted from southeast to northwest, resulting in the disappearance of geon 16 detrital zircon, the predominance of a combined Yavapai and Penokean population, and a subdued, but distinct, Algoman population (Fig. 2; Supplementary data, Table 3).

Baraboo Interval sediments are characteristically red due to the presence of hematite (Fig. 3A), but where quartzite was intruded and recrystallized by the Wolf River batholith or granite in the Wausau complex, hematite was reduced to magnetite, imparting a gray color to the quartzite (Fig. 3B and C).

Baraboo Interval siliciclastic rocks are among the most mature in the geological record, and, in this respect, are unique in Precambrian strata in the SLSR. Conglomerate contains quartz and ferricrete (or jasper) pebbles (Figure 3), clasts of underlying lithologies are absent, sandstone and siltstone are devoid of detrital feldspar, and shale contains kaolinite or its metamorphic equivalent, pyrophyllite (Southwick and Mossler, 1984; Medaris Jr. et al., 2003), all of which attest to the extreme mineralogical maturity of the strata. Chemically, the strata are equally mature, with pelitic layers having values of 97.5 to 99.0 for the Chemical Index of Alteration (CIA = $100 \times \text{molar Al}_2\text{O}_3 / (\text{Al}_2\text{O}_3 + \text{K}_2\text{O} + \text{Na}_2\text{O} + \text{CaO})$, compared to a value of 70.0 for average shale (Fig. 4; Supplementary data, Table 1). Such extreme mineralogical and chemical maturities are the result of complete removal of ferromagnesian minerals and feldspar from mature sub-Baraboo Interval paleosols across the region, which locally reach a thickness of ten meters (Driese and Medaris Jr., 2008). These paleosols developed under warm, humid climatic conditions, which are estimated to have been a mean annual temperature of 14.5 °C and a mean annual precipitation of 1180 mm/yr in the Baraboo Range (Medaris Jr. et al., 2017). An important corollary to these observations is that topographic relief must have been relatively subdued in the SLSR to allow for development of such mature paleosols

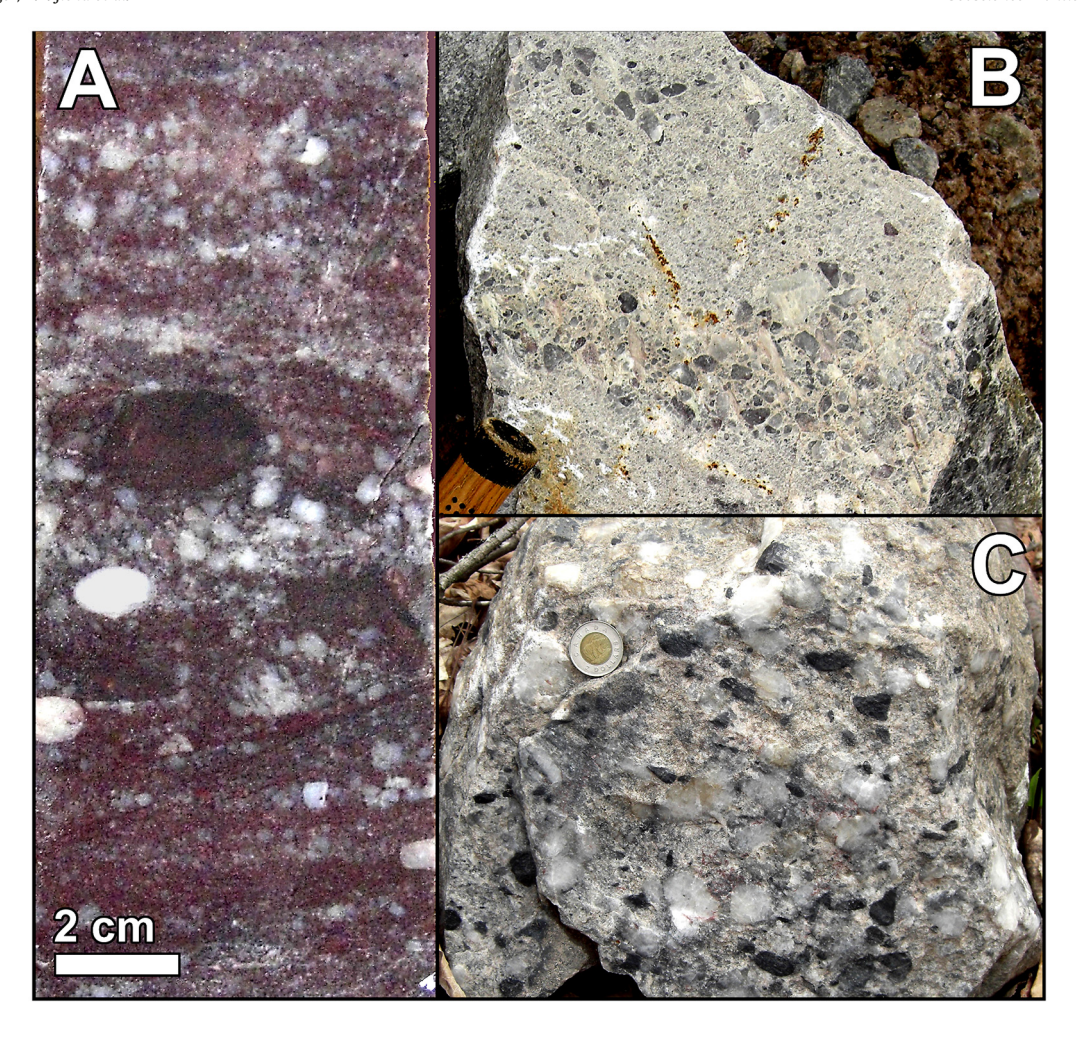


Fig. 3. Baraboo Interval quartz pebble conglomerates. A: Polished surface of drill core in Baraboo quartzite, 0.6 m above the unconformity; note the ferricrete pebble near the center of view. B: Waterloo quartzite with gray and white quartz pebbles; note the hammer handle for scale (lower left). C: Bedding surface in Thunder Mountain conglomerate; pebbles are quartz (white) and magnetite (black, formerly jasper); the coin is 2.7 cm in diameter.

and accompanying deposition of the supermature Baraboo Interval quartzites.

5. Geon 14 sedimentation: Baldwin conglomerate

Three occurrences of Proterozoic metasedimentary rocks, viz. the McCaslin quartzite, the Thunder Mountain quartzite, and the Baldwin conglomerate, are located at the northeastern margin of the Wolf River batholith, where all three are unconformable on Penokean volcanic rocks and are intruded by 1470 Ma Hager porphyry (Figure 5). Previously, these three sedimentary units were considered to belong to the Baraboo Interval, but we now recognize that the Baldwin conglomerate is a younger and compositionally less mature sedimentary deposit. The Baldwin conglomerate is polymictic (Fig.) and contains pebbles and cobbles of the underlying Penokean metavolcanic rocks (Waupee Formation) and gneiss (Macauley gneiss), all of which are set in an a medium— to coarse—grained arkosic matrix. In addition, cobbles of supermature quartzite are present (Fig. 6), presumably derived from the McCaslin and Thunder Mountain quartzites.

A relative probability plot for detrital zircon in the Baldwin conglomerate displays a predominant population with a minimum age peak at 1493 Ma and subsidiary populations with peaks at 1598, 1674, 1789, 1888, and 2690 Ma (Fig. 7; Supplementary data, Table 3). The four older peaks correlate with the Mazatzal, Yavapai, Penokean, and Algoman orogenies, and the geon 15 population probably reflects

contributions from the 1565–1506 Ma Wausau syenite–granite complexes, which are located 15 km west of the Wolf River batholith (Fig. 1). The MDA for the youngest statistically homogenous population of detrital zircon is 1458 ± 10 Ma (MSWD = 0.2; n=13), which overlaps within uncertainty with the age, 1470.5 ± 1.6 Ma, of the Hager granite porphyry that intrudes the conglomerate (DeWayne and Van Schmus, 2007). However, fifty-five detrital zircon grains have ages between 1522 and 1468 Ma, which is the age span for Wolf River magmatism in the region. This, and the location of the Baldwin conglomerate in the epizonal, ~1470 Ma part of the batholith, suggests that deposition of the conglomerate was approximately contemporaneous with emplacement (and possible eruption) of the northeastern part of the batholith at a shallow crustal level.

6. Geon 14 Metamorphism, metasomatism and deformation

In the western and northern areas of the SLSR, the Baraboo Interval Sioux quartzite and Barron quartzite are both flat–lying and nonconformable on Archean and Penokean basement, respectively (Fig. 1). In contrast, the remaining Baraboo Interval strata to the east and south are folded and nonconformable on Penokean and Yavapai basement. The flat–lying strata are unmetamorphosed and contain kaolinite, whereas the folded strata are recrystallized and contain pyrophyllite, which formed at ~300 °C through a reaction, such as:

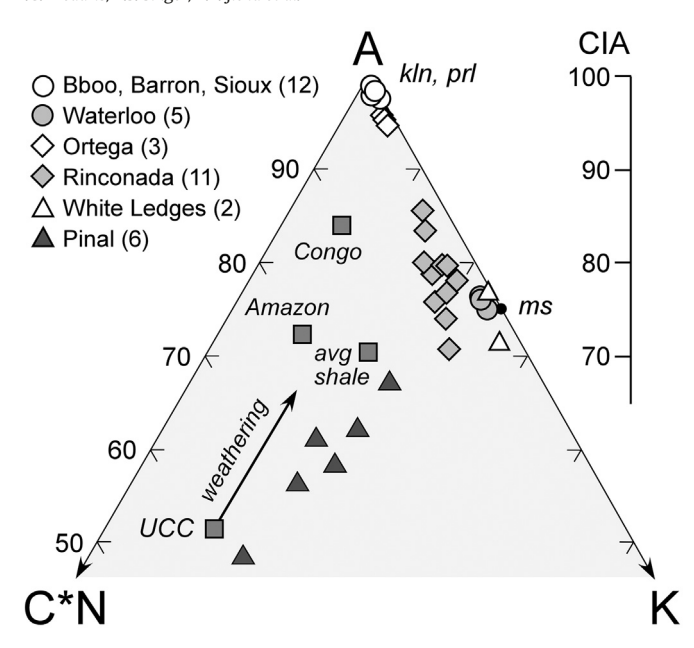


Fig. 4. Compositional plot for mudstones and siltstones in terms of molar Al_2O_3 (A), CaO (Ca*), Na₂O (N), and K₂O (K). The Baraboo, Barron, Sioux, and Waterloo samples are from the Baraboo Interval; the Waterloo metapelite has experienced K-metasomatism and plots near the composition of muscovite (ms). The Ortega metapelite and the Rinconada Formation are from the Hondo Group in northern New Mexico, the metasomatized White Ledges metapelite is from the Hess Canyon Group in southern Arizona, and the Pinal schist is from southern Arizona. The number of analyzed samples at each locality is indicated in parentheses. CIA, Chemical Index of Alteration (see text for explanation). Average upper continental crust (UCC) from Rudnick and Gao (2004); average shale and Amazon and Congo fine-grained particulates from Taylor and McLennan (1985).

$$Al_4Si_4O_{10}(OH)_8\,(kln) + 4SiO_2\,(qtz) = Al_4Si_8O_{20}(OH)_4\,(prl) + 2H_2O\,(V). \eqno(1)$$

At higher temperatures, pyrophyllite is stable in the presence of quartz up to \sim 385 °C (at a pressure of 2 kb).

In the Baraboo Range, hydrothermal veins at the base of the quartzite (Fig. 8) contain the mineral assemblage, diaspore + pyrophyllite + muscovite, which is stable between ~315 °C and ~ 365 °C (at 2 kb).

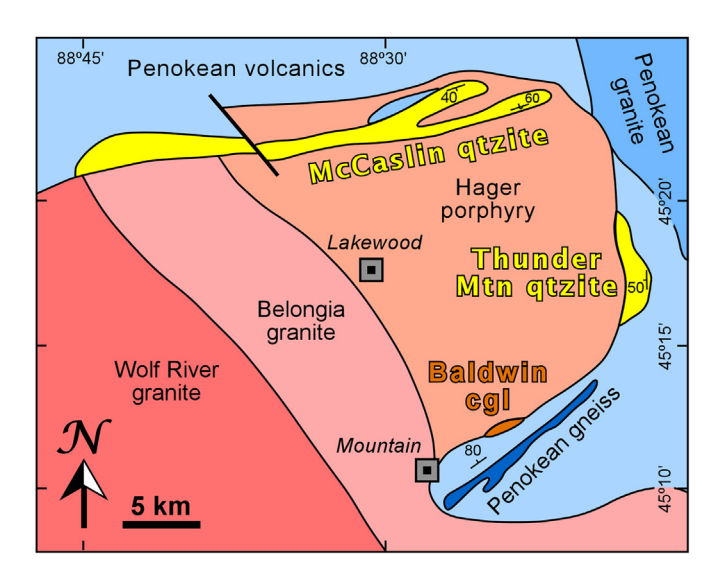


Fig. 5. Simplified geological map of Proterozoic rocks at the northeastern end of the Wolf River batholith, showing the outcrop distribution of the Baraboo Interval McCaslin and Thunder Mountain quartzites and the geon 14 Baldwin conglomerate (modified from Greenberg and Brown, 1984, Green, 1982). The Belongia granite and Hager porphyry (syenite and granite) are members of the 1470 Ma epizonal part of the batholith.



Fig. 6. Outcrop of polymictic Baldwin conglomerate, containing rounded pebbles of Waupee metavolcanic rocks (dark clasts), Penokean gneiss and granite (lighter clasts), and quartzite (white clasts, arrow); the coin is 2.7 cm in diameter.

Quartzite breccia high in the quartzite section contains the assemblage, quartz + kaolinite + muscovite, which combined with the compositions of fluid inclusions in quartz, constrains P-T conditions during brecciation to have been a maximum of $\sim\!2$ kb ($\sim\!7.5$ km) and 300 °C (Medaris Jr et al., 2002). T-P conditions of 300–385 °C and 2 kb for the regional metamorphic assemblage, pyrophyllite + quartz, are consistent with a surface heat flow of 110–140 mWm $^{-2}$, compared to an average continental surface heat flow of 65 mWm $^{-2}$.

Where Baraboo Interval sediments were intruded by granite, such as at the northeastern edge of the Wolf River batholith (Figs. 1 and 5) and in the Waterloo quartzite, where granite dikes, 0.3 to 1.2 m wide, intrude quartzite in the Michels quarry, andalusite crystallized in pelitic layers at temperatures above ~400 °C though a reaction, such as:

$$Al_4Si_8O_{20}(OH)_4$$
 (prl) = $6SiO_2$ (qtz) + $2Al_2SiO_5$ (and) + $2H_2O$ (V).

The absence of kyanite constrains recrystallization to have been at pressures below 2 to 4 kbar over a temperature range of 400 to 500 °C.

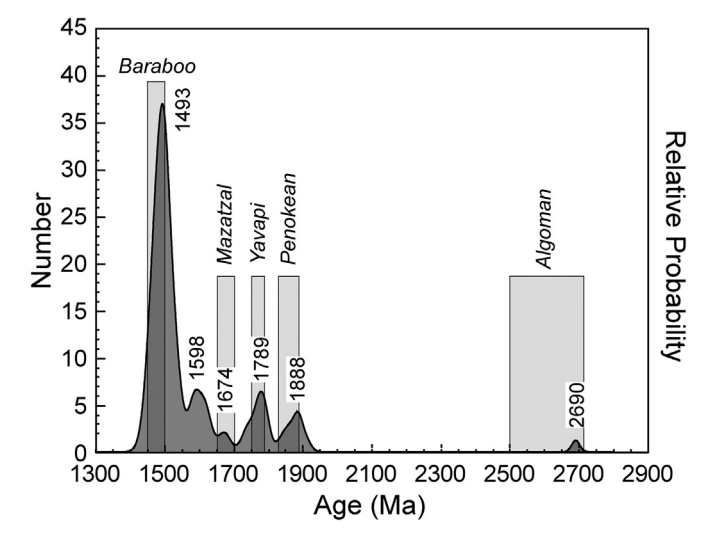


Fig. 7. Relative probability plot for detrital zircon in the Baldwin conglomerate; the age spans of orogenies in the southern Lake Superior region are indicated by the vertical bars.

Fold axes in Baraboo Interval sedimentary rocks are oriented generally ENE-WSW, for which finite strain analyses document a NW-SE tectonic shortening (Craddock and McKiernan, 2007). Finite strain magnitudes increase from the undeformed Sioux and Barron quartzites in the northwest to the folded Baraboo and Waterloo quartzites in the southeast. In the folded quartzites, the axial ratios of strain ellipsoids for quartz increase from 1.08:1:0.92 in the Flambeau quartzite in the northwest to 1.24:1:0.79 in the Baraboo quartzite to the southeast. The time of folding is constrained to have been between 1643 Ma, which is the MDA for the Waterloo quartzite, and 1470 Ma, the crystallization age of the Hager porphyry, which intrudes the synclinal structure of the McCaslin quartzite (Fig. 5). Although the Wolf River batholith is largely undeformed, the orientations of healed microcracks and planes of fluid inclusions in quartz record a NW-SE maximum horizontal stress for the region at ~1470 Ma (Jang et al., 1989; Jang and Wang, 1991), which is consistent with the strain regime for the folded quartzites.

Previously, a 1630 Ma thermal front was identified in the Penokean Province in northern Wisconsin, based on the distribution of ⁴⁰Ar/³⁹Ar cooling ages of mica in pre-Baraboo Interval basement (Fig. 1; Holm et al., 1998; Romano et al., 2000). North and west of this thermal front, mica in basement beneath the flat-lying Sioux and Barron quartzites has an age of 1760-1750 Ma, reflecting cooling and stabilization after the Yavapai orogeny. South and east of this front, mica in basement beneath folded quartzites has an age of 1614-1576 Ma, which records the effects of Mazatzal deformation and metamorphism. Because the 1.63 Ga thermal front in the basement coincides spatially with the distribution of flat-lying and folded quartzites, it was suggested that folding of Baraboo Interval quartzites was the result of Mazatzal deformation (Holm et al., 1998). However, although the mica ages clearly record Yavapai and Mazatzal recrystallization in the pre-Baraboo Interval basement, no isotopic ages were obtained from the Baraboo Interval strata themselves. As demonstrated above, Baraboo Interval sediments were deposited after 1643 Ma, and folding of the quartzites must therefore have been a post-Mazatzal event.

The relation between folding, metamorphism, and K-metasomatism is best illustrated in the Baraboo Range, which is the best exposed and most thoroughly investigated of the folded Baraboo Interval localities (Dalziel and Dott Jr., 1970; Medaris Jr. et al., 2003; Stewart et al., 2018). The Baraboo quartzite occurs in an asymmetric syncline, where it is nonconformable on a 1.75 Ga basement of rhyolite, granite, and diorite and is overlain conformably by the Seeley slate (Fig. 8). Quartzite and metapelite contain a restricted mineral assemblage of quartz + pyrophyllite + hematite, and because of this, few geochronologic methods are available to determine the age of recrystallization. However, muscovite, which was precipitated locally due to K-metasomatism promoted

by hydrothermal fluid flow along permeable channels in the syncline, can be dated by 40 Ar/ 39 Ar geochronometric methods. Such muscovite occurs at the unconformity at the base of the quartzite, in hydrothermal veins near the base of the quartzite, in a breccia zone in the upper part of the quartzite, and pervasively along axial plane cleavage in the Seeley slate that overlies quartzite (Fig. 8).

The crystallization of muscovite in all four settings was dated previously by application of the ${}^{40}\mathrm{Ar}/{}^{39}\mathrm{Ar}$ geochronometer, yielding geon 14 ⁴⁰Ar/³⁹Ar plateau ages in each instance (Medaris Jr et al., 2002; Medaris Jr. et al., 2003; Medaris Jr et al., 2009; Medaris Jr. and Singer, 2010). Here, we recalculate the ⁴⁰/³⁹Ar ages relative to the 28.201 Ma Fish Canyon sanidine standard (Kuiper et al., 2008), using the decay constants of Min et al. (2000) (Fig. 9; Supplementary data, Table 4). Plateau ages for muscovite are 1467 \pm 11 Ma in paleosol at the unconformity, 1478 ± 12 Ma in hydrothermal veins low in the quartzite section, and 1472 ± 3 Ma in breccia high in the quartzite section (Fig. 9). In the Seeley slate, which lies stratigraphically above the Baraboo quartzite (Fig. 8), three samples yield whole-rock ages of 1473 \pm 3, 1483 \pm 3, and 1493 ± 3 Ma (Fig. 9), and considering the low recrystallization temperature of the Seeley slate, 300–350 °C, it is likely that the whole-rock 40 Ar/ 39 Ar plateau ages approximate the time of muscovite growth in the slate. Elsewhere in the region, muscovite in the Waterloo metapelite, which also experienced K-metasomatism (Fig. 4), has a ⁴⁰Ar/³⁹Ar plateau age of 1465 \pm 5 Ma (Fig. 9). Muscovite in the Seeley slate is aligned parallel to axial-plane (slatey) cleavage (Fig. 10A), and muscovite in the Waterloo metapelite decorates crenulation cleavage (Fig. 10B). These muscovite textural features link K-metasomatism, recrystallization, and deformation, indicating that deformation in the Baraboo Range and in Waterloo quartzite was a geon 14 event, and suggesting that folding of other Baraboo Interval sedimentary rocks in the region was also a geon 14 tectonic phenomenon.

Rubidium, which follows potassium geochemically, was also locally introduced by hydrothermal fluid flow in folded Baraboo Interval strata. Relative to Upper Continental Crust (Rudnick and Gao, 2004), 96% Rb was added to Waterloo metapelite, 134% to Seeley slate, and 51% to Baraboo paleosol (calculated from data in Table 1 and Medaris Jr. et al., 2017). Nine samples of Baraboo paleosol define a Rb–Sr wholerock isochron age of 1336 \pm 75 Ma (Figs. 4 and 5 in Medaris Jr. et al., 2017), which is consistent with the $^{40}{\rm Ar}/^{39}{\rm Ar}$ results for muscovite, considering the different behavior and blocking temperatures for the two geochronologic systems.

Further evidence for geon 14 recrystallization of the Baraboo Interval (unrelated to K–metasomatism) is provided by folded pyrophyllite layers (metapelite) in the Baraboo Quartzite, which contain tiny grains (50–100 μ m) of neoblastic hematite (Fig. 10C). We measured (U–Th)/ He ages of multiple aliquots of this hematite, either as single crystals

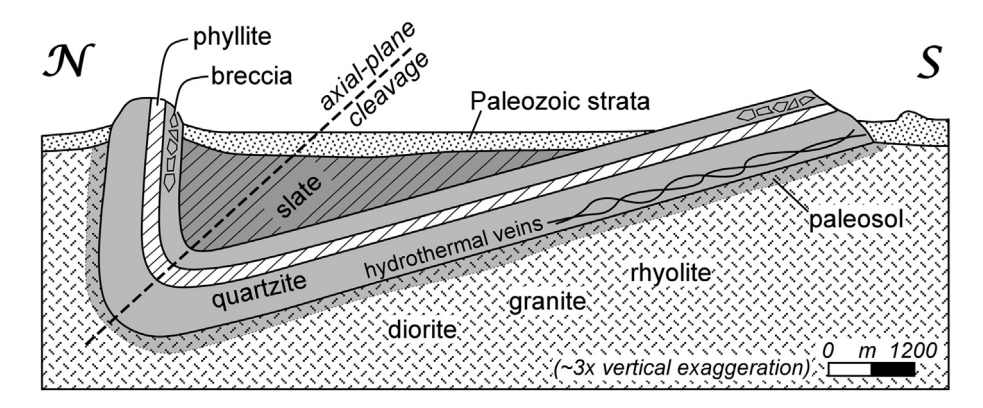
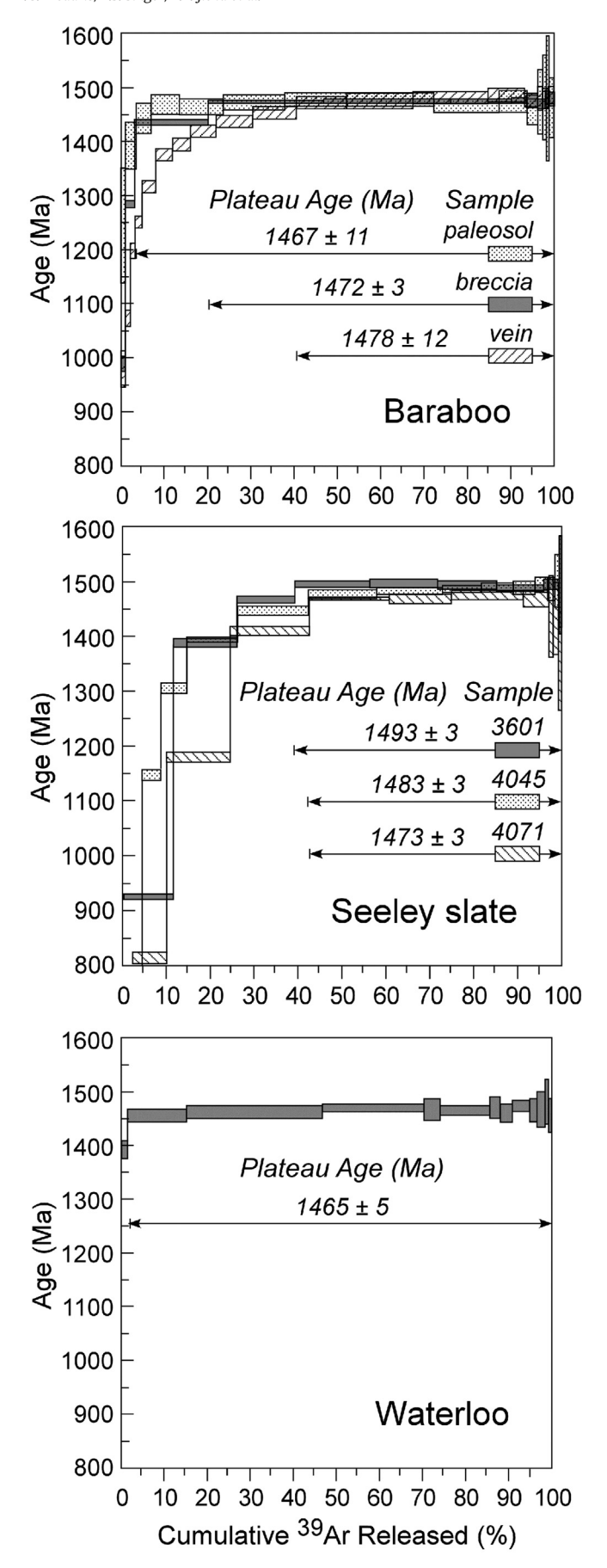


Fig. 8. Schematic cross-section of the Baraboo syncline, illustrating folding of the Baraboo quartzite and development of axial-plane cleavage in the Seeley slate and Baraboo phyllite (modified from Marshak et al., 2016). Geon 14 channelized fluid flow promoted K-metasomatism in paleosol, hydrothermal veins, and breccia. Rather than a single layer, the phyllite consists of several thin metasiltstone and metapelite layers high in the quartzite section. Several sub-Paleozoic sedimentary units, including dolomite, iron formation, quartzite, and slate (totaling ~600 m in thickness), that occur in the axis of the syncline above the Seeley slate are known only from drill core and are omitted from the cross-section.



or agglomerations of several crystallites with dimensions on the order of tens of μm using methods described in Evenson et al. (2014). Aliquots from several samples had low eU (U + 0.24*Th) of 1–2 ppm, resulting in relatively large uncertainties, and aliquots for some samples showed evidence for large U-losses (e.g., Hofmann et al., 2020) during lasing for He extraction, compared with unlased aliquots of the same samples. Here we report only results from aliquots from sample 17BQ15 that did not display this behavior, showed no systematic difference between age/composition ratios between low and intense lasing conditions, and had eU > 4 ppm. The mean age of hematite aliquots from this sample is 1411 ± 39 Ma (Fig. 11; Supplemental Table S5), which is slightly younger than those obtained for muscovite by $^{40} Ar/^{39} Ar$ geochronometry (1493–1465 Ma).

A third line of evidence for geon 14 recrystallization of the Baraboo Interval is provided by U-Th-total Pb dating by electron microprobe of monazite, small grains of which occur in trace amounts in the Seeley Slate in the Baraboo Range. These grains commonly have detrital cores overgrown by neoblastic rims that are elongated in the plane of axial cleavage (Fig. 12). Detrital monazite cores yielded Penokean and Archean dates, whereas monazite rims in five domains of two samples yielded dates of 1451, 1488, 1488, 1497, and 1528 Ma, with a weighted mean of 1502 \pm 30 Ma (Fig. 12; Supplementary data, Table 6). When the 1528 Ma age is excluded, one obtains a more statistically robust result of 1488 \pm 20 Ma (MSWD = 0.023, Chi-squared = 0.98). This date is within error of those provided by the $^{40}{\rm Ar}/^{39}{\rm Ar}$ and (U/Th)-He geochronologic methods and further substantiates the existence of geon 14 recrystallization in the southern Great Lakes region.

7. Geon 14 magmatism: Wolf River batholith

The Wolf River batholith was first identified by Van Schmus et al. (1975a) and subsequently investigated in detail by Anderson and Cullers (1978) and Anderson (1980). Because the Wolf River batholith plays an integral role in interpreting the early Mesoproterozoic evolution of the SLSR, its salient characteristics are summarized here. The batholith was originally classified as anorogenic, or A-type, but it is now known that emplacement of the batholith was coeval with regional metamorphism and folding, so the term, anorogenic, is inappropriate and has been abandoned.

The batholith contains anorthosite, monzonite (mangerite), and rapakivi granite and is a midcontinental member of the Anorthosite-Mangerite-Charnockite-Granite suite of igneous complexes that extends across much of southern Laurentia (Anderson, 1983). The batholith is predominantly granite, whose alkali feldspar–rich compositions contrast markedly with the plagioclase–rich compositions of Penokean quartz diorite–tonalite–granodiorite plutons in the region (Fig. 13A). The batholith includes four types of granitic rocks: a sequence of quartz syenite cumulate rocks, several intrusive monzogranite plutons, the Wolf River syenogranite–monzogranite pluton itself, and a group of differentiated syenogranite plutons (Fig. 13A). Three monzogranite plutons and the Wolf River pluton, which have mesozonal characteristics, have a composite U–Pb zircon age of 1476 \pm 2 Ma, whereas five differentiated syenogranite epizonal plutons have a composite age of 1470 \pm 1 Ma (DeWayne and Van Schmus, 2007).

The Wolf River plutons have ferroan chemical compositions, again in contrast to the Penokean plutons, which are magnesian (Fig. 13B).

Fig. 9. ⁴⁰Ar/³⁹Ar age spectra: Baraboo (upper panel), muscovite from quartz–muscovite metapaleosol, muscovite-pyrophyllite-diaspore hydrothermal vein, and quartz–muscovite-kaolinite breccia; Seeley slate (middle panel), whole rocks from quartz–muscovite-chlorite slate; Waterloo (lower panel), muscovite from quartz–muscovite-andalusite schist. Lengths of arrows indicate the steps included in the plateau age calculation for each sample.

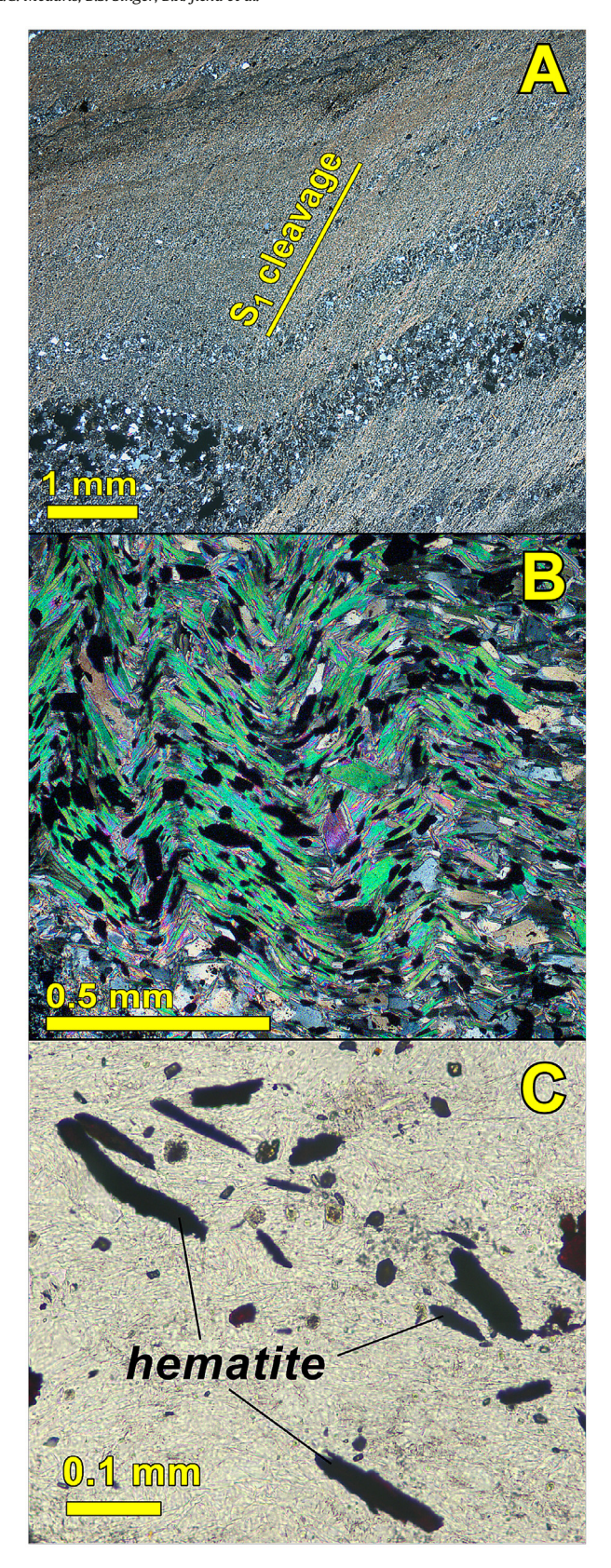


Fig. 10. A: Photomicrograph (crossed polarizers) of Seeley slate in the Baraboo Range, illustrating the alignment of fine–grained muscovite parallel to the plane of S₁ cleavage (slatey cleavage). B: Photomicrograph (crossed polarizers) of Waterloo metapelite in the Michels quarry, with crenulation cleavage illustrated by the orientation of muscovite grains. C: Photomicrograph (plane polarized light) of metapelite in the Baraboo Quartzite, showing neoblastic hematite grains in a matrix of fine-grained pyrophyllite.

Further differences are found in their alkali–lime indices (Peacock, 1931), with the Wolf River batholith being alkalic, having an index of 47, whereas the Penokean plutons are calc–alkalic, having an index of 60. The Wolf River plutons and the Penokean plutons both range from metaluminous to peraluminous, with the Wolf River plutons having a slightly higher mean value of Aluminum Saturation Index (ASI; Shand, 1927), 1.03 ± 0.06 , compared to that in the Penokean plutons, 0.98 ± 0.10 , where.

 $ASI = molecular Al_2O_3/(K_2O + Na_2O + CaO)$

Wolf River plutons in the 1476 Ma group are increasingly refractory from the oldest pluton (Wolf River granite, 1478 \pm 3 Ma) to the youngest (Red River granite, 1474 \pm 2 Ma), viz. an increase in Ca#, CaO/ (CaO + Na2O), from 0.22 to 0.41 and a decrease in Fe#, FeO*/ (FeO* + MgO), from 0.95 to 0.81 (Fig. 13B). In contrast, plutons in the 1470 Ma group are more differentiated, having a lower Ca# (0.13 to 0.28) and a higher Fe# (0.91 to 0.98) compared to the 1476 Ma group (Fig. 13B). These compositional differences between the older and younger groups of plutons are accompanied by differences in silica content, with the younger group containing >35% modal quartz and > 75 wt% SiO2 (Fig. 13B).

Major element, trace element, and Hf isotopic compositions are all consistent with a crustal source for the Wolf River batholith with little or no mantle input (Anderson and Cullers, 1978; Anderson, 1980; Goodge and Vervoort, 2006). Based on phase equilibria modelling, the plutons are thought to have been derived by partial melting of tonalitic to granodioritic crust at depths of 25 to 36 km, followed by emplacement of the 1470 Ma plutons at depths of 3.8 km or less (ibid.). The crustal derivation of the Wolf River batholith places important constraints on the tectonomagmatic scenario for the Baraboo orogeny, as discussed in Section 8.1.

8. Transcontinental extent of geon 14 orogenesis

Geon 14 orogenesis extends along the entire southern margin of Laurentia, different segments of which are referred to, from southwest to northeast, as the Picuris (Daniel et al., 2013), Baraboo (this paper),

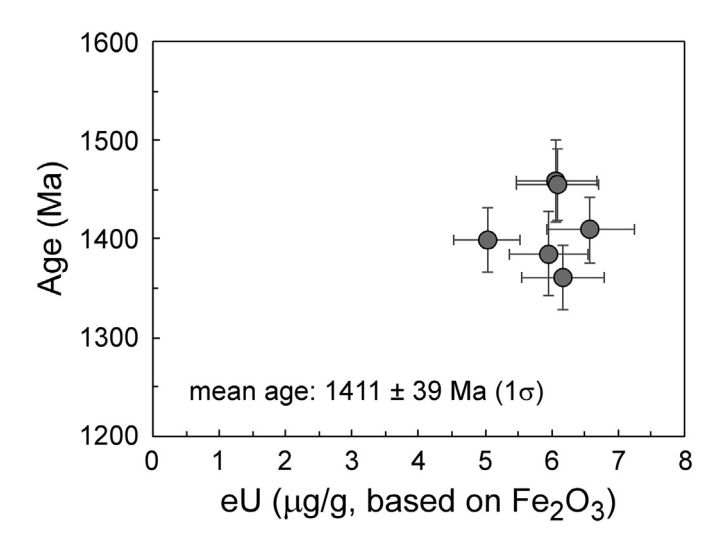


Fig. 11. (U—Th)/He ages of hematite in sample 17BQ15, plotted as a function of eU (U + 0.24° Th) concentration, as determined by Fe concentration of aliquot and assuming stoichiometric Fe₂O₃. Error bars on eU are shown as 10%, based on typical variation between microbalance– and Fe–determined masses of aliquots. Error bars on age are 2σ analytical precision.

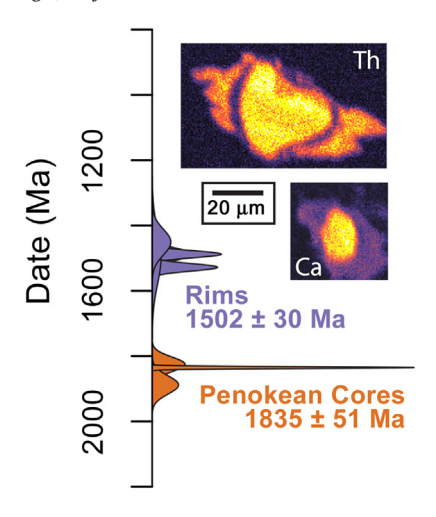


Fig. 12. Monazite dates from the Seeley slate. Each Gaussian peak represents one monazite date from a single compositional domain. Individual dates involve a single multipoint background analysis followed by multiple peak analyses. WDS maps (Th and Ca) are shown for two representative monazite grains.

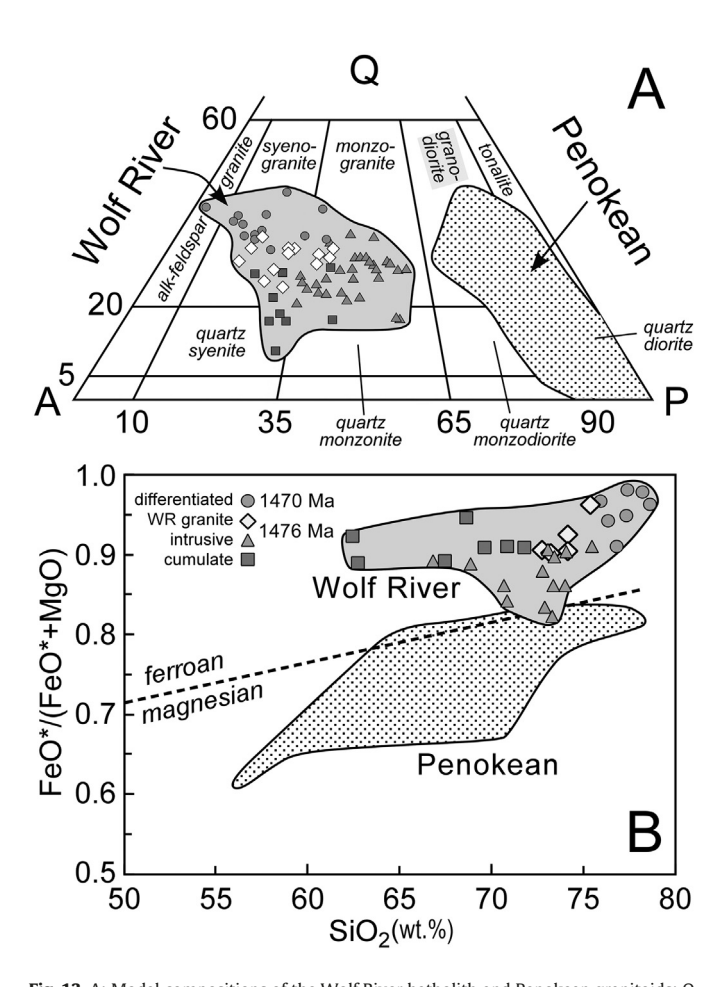


Fig. 13. A: Modal compositions of the Wolf River batholith and Penokean granitoids; Q, quartz; A, alkali feldspar; P, plagioclase. B: Discrimination of ferroan and magnesian granitoids in terms of Fe-index, FeO*/(FeO* + MgO), and wt% SiO₂ (plot after Frost and Frost, 2011; data from Anderson and Cullers, 1978, 1987).

and Pinware orogenies (Tucker and Gower, 1994; Heaman et al., 2004; Augland et al., 2015). This transcontinental orogenic belt was constructed on Penokean, Yavapai, Mazatzal, and Granite-Rhyolite basement and includes geon 14 folding and metamorphism of 1.7–1.4 Ga

siliciclastic sedimentary rocks and emplacement of 1.48–1.35 Ga ferroan granites (Fig. 14). We focus here on a comparison of the Baraboo and Picuris orogenies, which share many geological features, whereas discussion of the more complex Pinware orogeny, which was overprinted by the Grenville orogeny and contains remnants of 1.50–1.45 Ga volcanic arcs (Groulier et al., 2020), is beyond the scope of this investigation.

8.1. Geon 14 magmatism

One of the most striking features of this transcontinental orogenic belt is the widespread, 1.48-1.35 Ga emplacement of mostly ferroan granites in a 1600 km-wide swath across Laurentia (Fig. 14); such extensive igneous activity of this petrologic character has no Phanerozoic analogue and is considered to be unique to the Proterozoic (Anderson and Bender, 1989). The transcontinental extent of such granites was first recognized by Silver et al. (1977) and subsequently documented in detail by Anderson (1983), Anderson and Morrison (2005), Goodge and Vervoort (2006), and Bickford et al. (2015). Three groups of granites, all of which are rich in alkali feldspar, have been identified: a ferroan ilmenite series associated with anorthosite in the northeast (and including the Wolf River batholith in Wisconsin and the Sherman batholith in Wyoming), a ferroan magnetite series in the midcontinent and southwest, and a magnesian two-mica (peraluminous) series that transects the Yavapai and Mazatzal provinces, extending from central Colorado to New Mexico and Arizona (Fig. 15; Anderson and Bender, 1989; Anderson and Cullers, 1999; Anderson and Morrison, 2005). The differences among these three groups of granites are thought to reflect different conditions of melting of heterogeneous lower crust, combined with different oxidation conditions during crystallization. That the three groups of granite were derived from different crustal sources is demonstrated by the existence in the granites of a "Nd line" extending from Texas to Ohio that coincides with the boundary between the Mazatzal and Granite-Rhyolite Provinces (Fig. 14; Van Schmus et al., 2007). Nd model ages for granites on the southeastern side of this boundary reflect derivation from ~1500 Ma crust, whereas Nd model ages on the northwestern side reflect derivation from ≥1600 Ma crust, with model ages increasing to the northwest (Bickford et al., 2015).

It has been proposed that the geon 14 granites were generated by partial fusion of lower crust due to heating by underplating basaltic magmas (Anderson and Morrison, 2005; Goodge and Vervoort, 2006) and that such melting may have occurred in a continental back-arc environment (Whitmeyer and Karlstrom, 2007; Bickford et al., 2015). Such a tectonic setting is supported by trace element discriminant plots, in which samples of the Wolf River batholith and samples of the magnetite series and peraluminous series in the southwestern US plot in the "within plate" field, as defined by Pearce et al. (1984) (Fig. 16). Following generation by partial melting of lower continental crust, the granites were emplaced at middle to upper crustal levels, near and above the ductile-brittle transition, e.g., ≤3.8 km for the Wolf River batholith in Wisconsin (Anderson, 1980); ~11.3 km for the Signal batholith in Arizona (Nyman and Karlstrom, 1997); and 3.5–16.7 km for various plutons in California, Nevada, and Arizona (Anderson and Bender, 1989).

8.2. Post-Mazatzal deposition of supermature siliciclastic sediments

1.7–1.4 Ga siliciclastic sedimentary rocks are distributed across central and western Laurentia (Fig. 14), where those deposited on Penokean, Yavapai, and Mazatzal basement are folded (except for the Barron quartzite), but those deposited on Archean basement are not. Among these sedimentary rocks, quartzites of the post–Mazatzal *Baraboo Interval* in the midcontinent are distinctive for their extreme mineralogical and chemical maturity, as described in Section 4. Equally mature quartzites occur in the southwestern U.S., including the *Ortega quartzite* (Hondo Group, northern New Mexico; Jones III et al., 2011;

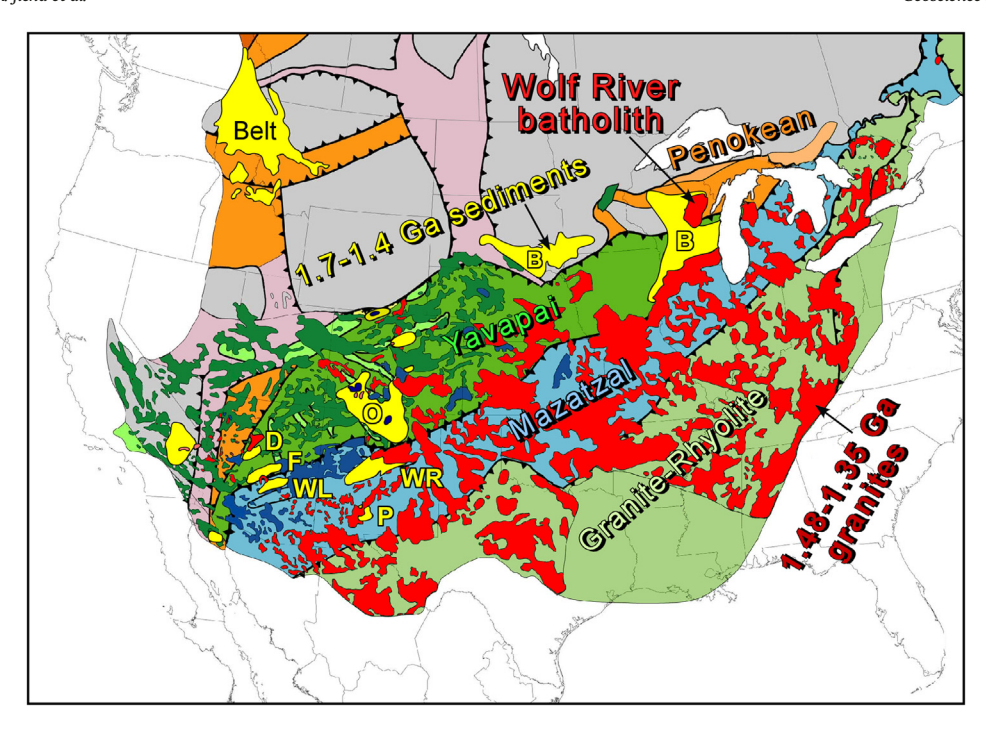


Fig. 14. Precambrian geological provinces in Laurentia at 1.3 Ga (modified from Whitmeyer and Karlstrom, 2007), including location of the Wolf River batholith, extent of 1.48–1.35 granites (in red), and distribution of 1.7–1.4 Ga siliciclastic sedimentary rocks (in yellow). Quartzite abbreviations: B, Baraboo Interval; D, Del Rio; F, Four Peaks; O, Ortega; WL, White Ledges; WR, White Ridge. Other abbreviation: P, Pinal schist. The Penokean, Yavapai, Mazatzal, and Granite-Rhyolite provinces are shown in shades of orange, green, blue, and gray green, respectively.

Daniel et al., 2013), the *Del Rio quartzite* (Little Chino Valley, central Arizona; Spencer et al., 2016), and the *Four Peaks quartzite* (Mazatzal Group, southern Arizona; Mako et al., 2015), which are located in the Yavapai province, and the *White Ridge quartzite* (Manzano Group, central New Mexico; Holland et al., 2020), and the *White Ledges quartzite* (Hess Canyon Group, southern Arizona; Doe et al., 2012), which are located in the Mazatzal province (Fig. 14). In New Mexico, the depositional age of the White Ridge quartzite is bracketed by the 1665–1660 Ma Seviletta metarhyolite below and the 1588 Ma Blue

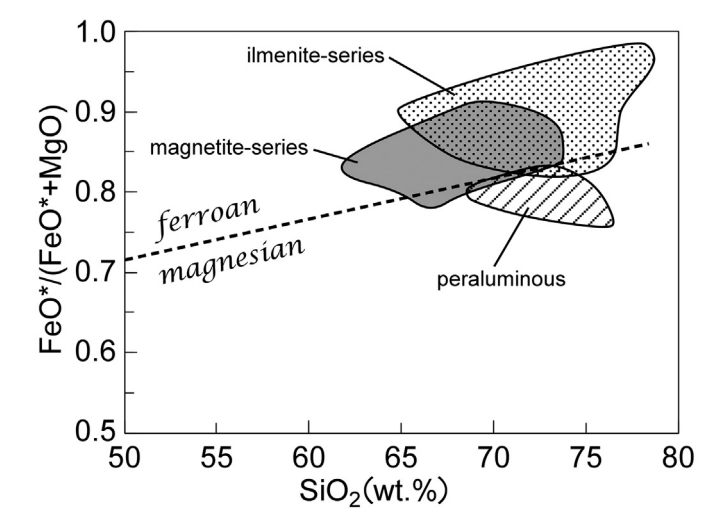


Fig. 15. Compositions of geon 14 granitic rocks in terms of Fe-index, Fe0*/(FeO* + MgO), and wt% SiO₂ (data from Anderson and Cullers, 1978; Anderson and Bender, 1989; Frost et al., 1999; Anderson and Morrison, 2005). The ilmenite-series includes the Sherman batholith (WY), the Lincoln granite (WY), and the Wolf River batholith (WI) (excluding cumulate rocks); the magnetite-series extends from New York to southern California along the Yavapai, Mazatzal, and Granite-Rhyolite provinces; the peraluminous-series transects the Yavapai and Mazatzal provinces in a belt from central Colorado to Arizona (see Anderson and Morrison, 2005).

Springs metarhyolite above (Holland et al., 2020). In Arizona, the White Ledges quartzite was deposited on 1657 Ma rhyolite (Doe et al., 2012), and the Four Peaks quartzite was also deposited on 1657 Ma rhyolite (Mako et al., 2015). These field relations demonstrate the late- or post-Mazatzal deposition of the quartzites.

Quartzites in the Yavapai province typically display prominent geon 17 probability peaks for detrital zircon, reflecting the influence of underlying Yavapai basement. Detrital zircon grains in the upper Ortega, middle Ortega, Del Rio, and Four Peaks quartzites yield age probability peaks at 1741, 1722, 1737, and 1742 Ma, respectively (Jones III et al., 2011; Mako et al., 2015; Spencer et al., 2016). However, each of these quartzites also contains a small, but significant, number of geon 16 detrital zircon grains and yield MDA values of 1719 Ma for the upper Ortega, 1717 Ma for the middle Ortega, 1715 to 1659 Ma for the Del Rio, and 1719 Ma for the Four Peaks quartzite.

In the Mazatzal Province, the White Ledges quartzite contains a detrital zircon population whose age characteristics are similar to those in quartzites in the Yavapai province (Doe et al., 2012). The lower and upper members of the quartzite yield age probability peaks at 1726 and 1773 Ma, respectively, and again, contain a small, but significant, number of geon 16 grains, e.g., 15 of 115 grains and 5 of 115, for which the MDA values are 1631 and 1698 Ma, respectively. Three samples of White Ridge quartzite, also located in the Mazatzal province, yield age probability peaks at 1676, 1667, and 1653 Ma, but in contrast to the White Ledges quartzite contain a higher proportion of geon 16 detrital zircon grains in each sample, e.g., 235 of 302 grains, 78 of 114 grains, and 96 of 116 grains (Holland et al., 2020). MDA values for these three quartzite samples are 1638, 1656, and 1648 Ma. Such detrital zircon data, along with the field relations, demonstrate that the supermature quartzites in the southwestern U.S. were deposited during the waning stages or after the 1.68-1.63 Ga Mazatzal orogeny, as defined by (Amato et al., 2008).

The quartzite sequences in New Mexico and Arizona, like those in the Baraboo Interval, progress upwards from fluvial facies to shoreface marine facies and are supermature mineralogically, consisting of quartz–jasper pebble conglomerate and quartz arenite, both of which

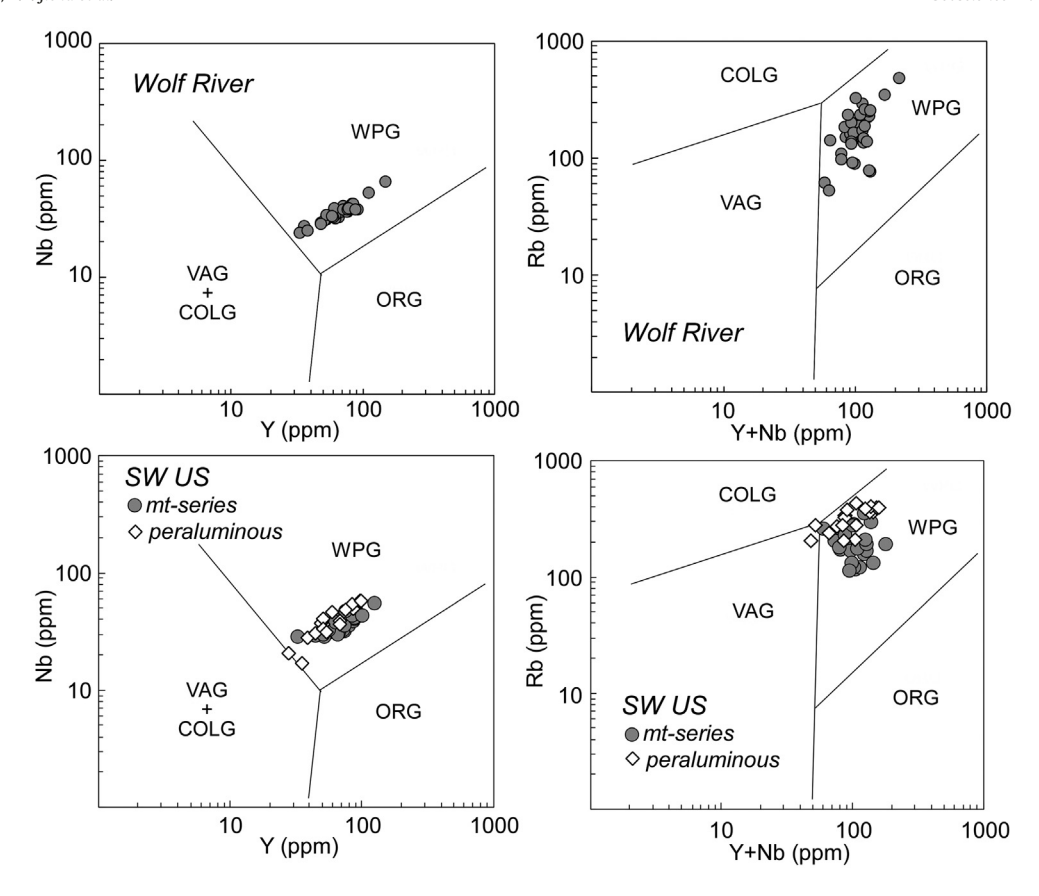


Fig. 16. Trace element discriminant plots for granites in the Wolf River batholith (upper panels; Anderson and Cullers, 1978) and geon 14 granitic plutons in the southwestern US (lower panels; Anderson and Bender, 1989); discriminant fields from Pearce et al. (1984). Abbreviations: COLG, collision granites; ORG, ocean ridge granites; VAG, volcanic arc granites; WPG, within plate granites.

are devoid of detrital feldspar. The absence of detrital feldspar is due to advanced chemical weathering, as seen in the paleosol beneath the Del Rio quartzite, where feldspar was completely removed during weathering (Spencer et al., 2016), as is also the case for paleosols beneath the Baraboo Interval. Additional evidence for the supermature nature of these sedimentary sequences is provided by the chemical composition of metapelite from the Ortega Formation, which has a Chemical Index of Alteration >95 and lies near the A apex in an A–C*N–K diagram (Fig. 4; Supplementary data, Table 1). In contrast to metapelite in the Ortega Formation, metapelite in the overlying Rinconada Formation is compositionally immature, having CIA values between 69 and 86 (Fig. 4; McLennan et al., 1995).

Metapelite from the White Ledges Formation is also supermature, although it has experienced K-metasomatism and plots near the composition of muscovite in the A-C*N-K diagram (Fig. 4; Supplementary data, Table 1), as does the composition of Waterloo metapelite, which also experienced K-metasomatism.

The Pinal schist in southernmost Arizona also contains geon 16 detrital zircon, with four samples yielding age probability peaks at 1690, 1685, 1675, and 1650 Ma (Bickford et al., 2019). However, in contrast to the supermature quartzites in New Mexico and Arizona, the Pinal schist is relatively immature, having been derived from quartz wacke, feldspathic wacke, and lithic wacke, whose CIA values range from 49 to 68 (Fig. 4; Meijer, 2014; Bickford et al., 2019). These immature siliciclastic sedimentary rocks are thought to have been deposited in a forearc–subduction complex related to a Mazatzal arc terrane (Meijer, 2014).

8.3. Geon 14 sedimentation

Siliciclastic sedimentation in the southwestern U.S. was associated with geon 14 regional metamorphism, deformation, and plutonism, as

it was in the SLSR. In the Picuris Mountains of New Mexico (Yavapai Province), the Pilar Formation in the Trampas Group contains a 1488 \pm 6 Ma metatuff layer, and detrital zircon in the overlying Piedra Lumbre Formation has a minimum age peak of 1475 Ma (Daniel et al., 2013). The Marqueñas Formation, which is separated from the Trampas Group by a ductile shear zone, has a minimum age peak of 1472 Ma for detrital zircon in the basal metaconglomerate and 1471 Ma for detrital zircon in overlying quartzite (Daniel et al., 2013). Two additional samples from the upper Marqueñas Formation have age probability peaks at 1479 and 1457 Ma and MDA values of 1477 \pm 13 and 1453 \pm 10 Ma, respectively (Jones III et al., 2011).

Geon 14 detrital zircon has also been identified in the Hess Canyon Group (Mazatzal province) of southcentral Arizona, where detrital zircon from the uppermost Yankee Joe Formation has a minimum age peak at 1495 Ma, and three samples from the overlying Blackjack Formation have minimum age peaks at 1515, 1499, and 1488 Ma (Doe et al., 2012). The Blackjack Formation was intruded by the 1436 \pm 2 Ma Ruin granite, which constrains deposition of the Hess Canyon Group to have been between 1488 and 1436 Ma. In the nearby Four Peaks area (Yavapai province), the MDA for the "upper pelite" in the stratigraphic section is 1566 \pm 14 Ma, and the pelite is intruded by the 1449 \pm 13 El Oso granite (Mako et al., 2015).

8.4. Geon 14 regional metamorphism and deformation

In the Yavapai Province in northern and central Colorado, biotite and muscovite have 40 Ar/ 39 Ar ages of ~1.4 Ga, and hornblende yields a range of ages from 1.7 to 1.4 Ga, reflecting regional greenschist facies metamorphism at temperatures of 300–500 °C (Shaw et al., 2005). In the classic Al₂SiO₅ triple point terrane in northern New Mexico (Grambling, 1981), Lu–Hf ages for garnet from amphibolite facies lithologies in the

Hondo and Trampas Groups record three stages of recrystallization and deformation at 1456–1450 Ma, 1419–1405 Ma, and < 1400 Ma (Aronoff et al., 2016), and a more recent evaluation of Lu–Hf and Sm–Nd data reveals protracted garnet growth over 50–80 Ma to ca. 1350 Ma (Bollen et al., 2019). Geon 14 metamorphic P–T–t paths passed in the vicinity of the $\rm Al_2SiO_5$ triple point at \sim 4 kb and \sim 500 °C (Williams and Karlstrom, 1996), at which stage the Hondo and Trampas Groups were buried to a depth of \sim 15 km and recrystallized under the influence of a transient, elevated geotherm (\sim 33 °C/km), corresponding to P–T conditions associated with a high T/P metamorphic field gradient. From the perspective of a steady–state geotherm, a temperature of 500 °C at a depth of 15 km would require a surface heat flow of 100 mWm $^{-2}$, which is similar to the geon 14 surface heat flow of 110–140 mWm $^{-2}$ estimated for the SLSR (Section 6).

9. Discussion

A distinctive aspect of the Mesoproterozoic Picuris and Baraboo orogenies is the widespread distribution of ferroan granites of crustal derivation, in contrast to the subduction–related tonalites and granodiorites that are characteristic of the Archean Algoman and Paleoproterozoic Penokean orogenies. The granite magmas were generated by partial fusion of lower continental crust and subsequently emplaced near and above the brittle–ductile transition at middle to upper crustal depths between 16 and 4 km (Anderson, 1980; Anderson and Bender, 1989; Shaw et al., 2005), where the granites contributed advective heat that promoted regional metamorphism.

The heat flux responsible for partial melting of the lower continental crust is thought to have been provided by mantle–derived basaltic melts that underplated the continental crust. Evidence for such mantle melts is found in 2.1–1.7 Ga spinel peridotite xenoliths in the Navajo Volcanic Field in the Colorado Plateau, which contain clinopyroxene that has a Sm–Nd isochron age of 1439 \pm 55 Ma, indicating mantle melt production and isotopic resetting at that time (Marshall et al., 2017). In addition, lower crustal mafic xenoliths in the Navajo Volcanic Field have zircon crystallization ages of 1435–1430 Ma (Crowley et al., 2006), providing a further link between mafic magmatism and granite magmatism at 1.4 Ga.

It has been proposed that the Picuris-Baraboo terrane represents a continental backarc plateau that formed in response to transpressional convergence along the southern margin of Laurentia, accompanied by the accretion of outboard volcanic arcs (Shaw et al., 2005; Bickford et al., 2015; Holland et al., 2020). Little evidence for such volcanic arcs remains, however, perhaps having been removed during the ~1.3 Ga rifting and breakup of Nuna or the later Neoproterozoic rifting of Rodinia, although the Pinal schist in southern Arizona, which was deposited in a forearc-subduction environment, may be a remaining fragment of such an arc.

Mantle melting, continental underplating, and crustal melting are commonly ascribed to decompression melting in an extensional setting. However, such melting and underplating in the Baraboo-Picuris orogen were apparently associated with transpression and crustal shortening, rather than extension. One possible solution to this enigma could be delamination, which promoted upwelling and melting of mantle and underplating of continental crust beneath the backarc plateau (Holland et al., 2020). Alternatively, a shallow-dipping, subducting slab undergoing dehydration may have existed beneath the plateau. Such dehydration could trigger melting in the overlying mantle, thereby removing extension as a requirement for mantle melting, and a shallow dip of the subducting slab could explain the great width of ferroan magmatism.

10. Conclusions

The geon 14 Baraboo orogeny is the penultimate Precambrian tectonometamorphic event in the SLSR of Laurentia. Its defining features include emplacement of the ferroan Wolf River batholith, NW–SE crustal shortening and folding of Baraboo Interval sedimentary rocks,

regional greenschist facies metamorphism under the influence of an elevated geotherm, and local deposition of arkosic, polymictic conglomerate. These characteristics are attributed to partial melting of the mantle, underplating and heating of continental crust by the resulting basaltic melts, generation of ferroan granitic magmas by partial melting of lower continental crust, and subsequent emplacement of such granites in the middle to upper crust, where advective heating promoted regional high T-P metamorphism. The Baraboo orogeny provides a midcontinental link between the Picuris orogeny to the southwest and the Pinware orogeny to the northeast, thus completing the extent of this major geon 14 orogenic belt for 5000 km along the southern margin of Laurentia.

Supplementary data to this article can be found online at https://doi.org/10.1016/j.gsf.2021.101174.

Declaration of Competing Interest

The authors declare that they have no known competing financial interests or personal relationships that could have appeared to influence the work reported in this paper.

Acknowledgements

We thank Chloe Bonamici and Michael Doe for contributing samples of Ortega metapelite and White Ledges metapelite. Detrital zircon analyses were funded in part by the USGS National Cooperative Geologic Mapping Program under award G16AC00143 (2016) to EKS. Support for the Arizona LaserChron Center, where detrital zircon analyses of samples 07ES15 and 05ES15 were performed, was provided by NSF-EAR 1649254. Support for monazite geochronology was partially provided by an Institute for Lake Superior Geology student research grant and NSF-EAR 0620101 to AVL. Thanks to Zhan Peng for assistance with geochronology in the CSUN Laser Laboratory and to Uttam Chowdhury for (U-Th)/He analytical assistance in the Arizona Radiogenic Helium Dating Laboratory. We also thank J. A. Muldur and M. E. Bickford for providing constructive reviews that improved the manuscript.

References

Allaz, J.M., Williams, M.L., Jercinovic, M.J., Goemann, K., Donovan, J., 2019. Multipoint background analysis: gaining precision and accuracy in microprobe trace element analysis. Microsc. Microanal. 25, 30–46. https://doi.org/10.1017/s14319276180 15660

Amato, J.M., Boullion, A.O., Serna, A.M., Anders, A.E., Farmer, G.L., Gehrels, G.E., Wooden, J.L., 2008. Evolution of the Mazatzal province and the timing of the Mazatzal orogeny: Insights from U-Pb geochronology and geochemistry of igneous and metasedimentary rocks in southern New Mexico. Geol. Soc. Am. Bull. 120, 328–346. https://doi.org/10.1130/B26200.1.

Anderson, J.L., 1980. Mineral equilibria and crystallization conditions in the late Precambrian Wolf River rapakivi massif. Wisconsin. Am. J. Sci. 280, 245–256. https://doi.org/10.2475/ais.280.4.289.

Anderson, J.L., 1983. Proterozoic anorogenic granite plutonism of North America. In: Medaris, L.G., Byers, C.W., Mickelson, D.M., Shanks, W.C. (Eds.), Proterozoic Geology: Selected Papers from an International Proterozoic Symposium. Geol. Soc. Am. Mem 161, pp. 133–154. https://doi.org/10.1130/mem161-p133.

Anderson, J.L., Bender, E.E., 1989. Nature and origin of Proterozoic A-type granitic magmatism in the southwestern United States of America. Lithos 23, 19–52. https://doi.org/10.1016/0024-4937(89)90021-2.

Anderson, J.L., Cullers, R.L., 1978. Geochemistry and evolution of the Wolf River Batholith, a late Precambrian rapakivi massif in north Wisconsin, U.S.A. Precambrian Res. 7, 287–324. https://doi.org/10.1016/0301-9268(78)90045-1.

Anderson, J.L., Cullers, R.C., 1987. Crust–enriched, mantle–derived tonalites in the Early Proterozoic Penokean orogen of Wisconsin. J. Geol. 95, 139–154. http://jstor.org/stable/30063804.

Anderson, J.L., Cullers, R.L., 1999. Paleo- and Mesoproterozoic granite plutonism of Colorado and Wyoming. Rocky Mountain Geol. 34, 149–164. https://doi.org/10.2113/34.2.149.

Anderson, J.L., Morrison, J., 2005. Ilmenite, magnetite, and peraluminous Mesoproterozoic anorogenic granites of Laurentia and Baltica. Lithos 80, 45–60. https://doi.org/ 10.1016/j.lithos.2004.05.008.

Anderson, J.L., Cullers, R.L., Van Schmus, W.R., 1980. Anorogenic metaluminous and peraluminous granite plutonism in the Mid-Proterozoic of Wisconsin, USA. Contrib. Mineral. Petrol. 74, 311–328. https://doi.org/10.1007/BF00371700.

- Aronoff, R.F., Andronicos, C.L., Vervoort, J.D., Hunter, R.A., 2016. Redefining the metamorphic history of the oldest rocks in the southern Rocky Mountains. Geol. Soc. Am. Bull. 128, 1207–1227. https://doi.org/10.1130/B31455.1.
- Augland, L.E., Moukhsil, A., Soldadi, F., Indares, A., 2015. Pinwarian to Grenvillian magmatic evolution in the central Grenville Province: new constraints from ID-TIMS U-Pb ages and coupled Lu-Hf S-MC-ICP-MS data. Can. J. Earth Sci. 52, 701-721. https://doi.org/10.1139/cjes-2014-0232.
- Bickford, M.E., Wooden, J.L., Bauer, R.L., 2006. SHRIMP study of zircons from Early Archean rocks in the Minnesota River Valley: implications for the tectonic history of the Superior Province. Geol. Soc. Am. Bull. 118, 94–108. https://doi.org/10.1130/B25741.1.
- Bickford, M.E., Van Schmus, W.R., Karlstrom, K.E., Muellerd, P.A., Kamenov, G.D., 2015. Mesoproterozoic trans-Laurentian magmatism: a synthesis of continent-wide age distributions, new SIMS U-Pb ages, zircon saturation temperatures, and Hf and Nd isotopic compositions. Precambrian Res. 265, 286–312. https://doi.org/10.1016/j. precamres.2014.11.024.
- Bickford, M.E., Mueller, P.A., Condie, K.C., Hanan, B.B., Kamenov, G.G., 2019. Ages and Hf isotopic compositions of detrital zircons in the Pinal schist, southern Arizona, USA: Provenance, tectonic setting, and evidence for pre-1.7 Ga crust in SW Laurentia. Precambrian Res. 331. https://doi.org/10.1016/j.precamres.2019.105374 Article 105374.
- Black, L.P., Kamo, S.L., Allen, C.M., Davis, D.W., Aleinikoff, J.N., Valley, J.W., Mundil, R., Campbell, I.H., Korsch, R.J., Williams, I.S., Foudoulis, C., 2004. Improved Pb-206/U-218 microprobe geochronology by the monitoring of a trace-element-related matrix effect; SHRIMP, ID-TIMS, ELA-ICP-MS and oxygen isotope documentation for a series of zircon standards. Chem. Geol. 205, 115–140. https://doi.org/10.1016/j.chemgeo.2004.01.003.
- Bollen, E.M., Stowell, H.H., Aronoff, R.F., Schwartz, J.J., 2019. Garnet Sm-Nd and Lu-Hf ages from the Picuris orogeny: understanding their meaning using trace element zoning. Geol. Soc. Am., Abstr. with Programs, v 51. https://doi.org/10.1130/abs/2019AM-335903 Abstr. no. 11–11.
- Craddock, J.P., McKiernan, A.W., 2007. Tectonic implications of finite strain variations in Baraboo-interval quartzites (ca. 1700 Ma), Mazatzal orogen, Wisconsin and Minnesota, USA. Precambrian Res. 156, 175–194. https://doi.org/10.1016/j.precamres. 2006.03.010.
- Craddock, J.P., Malone, D.H., Porter, R., Compton, J., Luczaj, J., Konstantinou, A., Day, J.E., Johnston, S.T., 2017. Paleozoic reactivation structures in the Appalachian-Ouachita-Marathon foreland: Far-field deformation across Pangea. Earth-Sci. Rev. 169, 1–34. https://doi.org/10.1016/j.earscirev.2017.04.002.
- Craddock, J.P., Malone, D.H., Schmitz, M.D., Gifford, J.N., 2018. Strain variations across the Proterozoic Penokean Orogen, USA and Canada. Precambrian Res. 318, 25–69. https://doi.org/10.1016/j.precamres.2018.09.004.
- Crowley, J.L., Schmitz, M.D., Bowring, S.A., Williams, M.L., Karlstrom, K.E., 2006. U-Pb and Hf isotopic analysis of zircon in lower crustal xenoliths from the Navajo volcanic field: 1.4 Ga mafic magmatism and metamorphism beneath the Colorado Plateau. Contrib. Mineral. Petrol. 151, 313–330. https://doi.org/10.1007/s00410-006-0061-z.
- Dalziel, I.W.D., Dott Jr., R.H., 1970. Geology of the Baraboo District, Wisconsin. Wisc. Geol. Nat. Hist. Surv., Inf. Circ 14 164 pp. https://wenhs.wisc.edu/pubs/000264/.
- Daniel, C.G., Pfeifer, L.S., Jones III, J.V., McFarlane, C.M., 2013. Detrital zircon evidence for non-Laurentian provenance, Mesoproterozoic (ca. 1490–1450) deposition and orogenesis in a reconstructed orogenic belt, northern New Mexico, USA: defining the Picuris orogeny. Geol. Soc. Am. Bull. 125, 1423–1441. https://doi.org/10.1130/ b30804.1.
- DeWayne, T.J., Van Schmus, W.R., 2007. U-Pb geochronology of the Wolf River batholith, north-central Wisconsin: evidence for successive magmatism between 1484 Ma and 1468 Ma. Precambrian Res. 157, 215–234. https://doi.org/10.1016/j.precamres.2007. 02 018
- Doe, M.F., Jones III, J.V., Karlstrom, K.E., Thrane, K., Frei, D., Gehrels, G., Pecha, M., 2012. Basin formation near the end of the 1.60–1.45 Ga tectonic gap in southern Laurentia: Mesoproterozoic Hess Canyon Group of Arizona and implications for *ca.* 1.5 Ga supercontinent configurations. Lithosphere 4, 77–88. https://doi.org/10.1130/L160.1.
- Dott Jr., R.H., 1983. The Proterozoic red quartzite enigma in the north-central U.S.: Resolved by plate collision? In:Medaris, L.G.Jr. (Ed), Early Proterozoic Geology of the Great Lakes region. Geol. Soc. Am. Mem. 160, 129–141.
- Driese, S.G., Medaris Jr., L.G., 2008. Evidence for biological and hydrological controls on the development of a Paleoproterozoic paleoweathering profile in the Baraboo Range, Wisconsin, U.S.A. J. Sediment. Res. 78, 443–457. https://doi.org/10.2110/ isr.2008.051.
- Evenson, N.S., Reiners, P.W., Spencer, J.E., Shuster, D.L., 2014. Hematite and Mn oxide (U-Th)/He dates from the Buckskin-Rawhide detachment system, western Arizona: Gaining insights into hematite (U-Th)/He systematics. Amer. J. Sci. 314, 1373–1435. https://doi.org/10.2475/10.2014.01.
- Freiburg, J.T., Holland, M.E., Malone, D.H., Malone, S.J., 2020. Rodinian rifting in the Illinois Basin: detrital zircon geochronology of basal Cambrian strata. J. Geol. 128, 303–317. https://doi.org/10.1086/708432.
- Frost, C.D., Frost, R., 2011. On ferroan (A-type) granitoids: their compositional variability and modes of origin. J. Petrol. 52, 39–53 doi:petrology/egq070.
- Frost, C.D., Frost, B.R., Chamberlain, K.R., Edwards, B.R., 1999. Petrogenesis of the 1.43 Ga Sherman batholith, SE Wyoming, USA: a reduced, rapakivi–type anorogenic granite. J. Petrol. 40, 1771–1802. https://doi.org/10.1093/petroj/40.12.1771.
- Gehrels, G.E., Pecha, M., 2014. Detrital zircon U–Pb geochronology and Hf isotope geochemistry of Paleozoic and Triassic strata of western North America. Geosphere 10, 49–65. https://doi.org/10.1130/GE00889.1.
- Gehrels, G.E., Valencia, V., Pullen, A., 2006. Detrital zircon geochronology by Laser-Ablation Multicollector ICPMS at the Arizona LaserChron Center. In: Loszewski, T., Huff, W. (Eds.), Geochronology: Emerging Opportunities, p. 11 Paleontology Society Short Course. Paleontol. Soc. Pap. 10 pp.

- Gehrels, G.E., Valencia, V., Ruiz, J., 2008. Enhanced precision, accuracy, efficiency, and spatial resolution of U-Pb ages by laser ablation–multicollector–inductively coupled plasma–mass spectrometry. Geochem. Geophys. Geosyst. 9, Q03017. https://doi.org/10.1029/2007GC001805
- Goodge, J.W., Vervoort, J.D., 2006. Origin of Mesoproterozoic A-type granites in Laurentia: Hf isotope evidence. Earth Planet. Sci. Lett. 243, 711–731. https://doi.org/10.1016/j.epsl.2006.01.040.
- Grambling, J.A., 1981. Kyanite, and alusite, sillimanite, and related mineral assemblages in the Truchas Peaks region, New Mexico. Amer. Miner. 66, 702–722. http://www. minsocam.org.ezproxy.library.wisc.edu/MSA/AmMin/TOC/.
- Green, J.C., 1982. Geology of Keweenawan extrusive rocks. In: Wold, R.J., Hinze, W.J. (Eds.), Geology and Tectonics of the Lake Superior Basin. Geol. Soc. Am. Mem. 156, 47–82.
- Greenberg, J.K., Brown, B.A., 1984. Bedrock geology of Wisconsin, northeast sheet. Wisc. Geol. Nat. Hist. Sur. M082.
- Groulier, P.-A., Indares, A., Dunning, G., Moukhsil, A., 2020. Andean style 1.50–1.35 Ga arc dynamics in the Southeastern Laurentian margin: the rifting and reassembly of Quebecia. Terra Nova 32, 450–457. https://doi.org/10.1111/ter.12482.
- Heaman, L.M., Gower, C.F., Perreault, S., 2004. The timing of Proterozoic magmatism in the Pinware terrane of Southeast Labrador, easternmost Quebec and Northwest Newfoundland. Can. J. Earth Sci. 41, 127–150. https://doi.org/10.1139/e03-088.
- Hinze, W.J., Allen, D.J., Braile, L.W., Mariano, J., 1997. The Midcontinent Rift system: a major Proterozoic continental rift. Geol. Soc. Am. Sp. Pap. 312, 7–35. https://doi.org/ 10.1130/0-8137-2312-4.7.
- Hofman, H.J., 1990. Precambrian time units and nomenclature the geon concept. Geology 18, 340–341. https://doi.org/10.1130/0091-7613(1990)018<0340:PTUANT>2.3. CO:2.
- Hofmann, F., Treffkorn, J., Farley, K.A., 2020. U-loss associated with laser-heating of hematite and goethite in vacuum during (U-Th)/He dating and prevention using high O_2 partial pressure. Chem. Geol. 532. https://doi.org/10.1016/j.chemgeo.2019.119350 article 119350.
- Holland, M.E., Grambling, T.A., Karlstrom, K.E., Jones III, J.V., Nagotko, K.N., Daniel, C.G., 2020. Geochronologic and Hf-isotope framework of Proterozoic rocks from central New Mexico, USA: Formation of the Mazatzal crustal province in an extended continental margin arc. Precambrian Res. 347. https://doi.org/10.1016/j.precamres.2020. 105820 article 105820.
- Holm, D., Schneider, D., Coath, C.D., 1998. Age and deformation of Early Proterozoic quartzites in the southern Lake Superior region: implications for extent of foreland deformation during final assembly of Laurentia. Geology 26, 907–910. https://doi. org/10.1130/0091-7613(1998)026<0907;aadoep>2.3.co;2.
- Holm, D.K., Van Schmus, W.R., MacNeill, L.C., Boerboom, T.J., Schweitzer, D., Schneider, D., 2005. U-Pb zircon geochronology of Paleoproterozoic plutons from the northern midcontinent, USA: evidence for subduction flip and continued convergence after geon 18 Penokean orogenesis. Geol. Soc. Am. Bull. 117, 259–275. https://doi.org/ 10.1130/B25395.1.
- Holm, D.K., Anderson, R., Boerboom, T.J., Cannon, W.F., Chandler, V., Jirsa, M., Miller, J., Schneider, D.A., Schulz, K.J., Van Schmus, W.R., 2007a. Reinterpretation of Paleoproterozoic accretionary boundaries of the north-central United States based on a new aeromagnetic-geologic compilation. Precambrian Res. 157, 71–79. https:// doi.org/10.1016/j.precamres.2007.02.023.
- Holm, D.K., Schneider, D.A., Rose, S., Mancuso, C., McKenzie, M., Foland, K.A., Hodges, K.V., 2007b. Proterozoic metamorphism and cooling in the southern Lake Superior region, North America, and its bearing on crustal evolution. Precambrian Res. 157, 106–126. https://doi.org/10.1016/j.precamres.2007.02.012.
- Holm, D., Medaris Jr., L.G., McDannell, K.T., Schneider, D.A., Schulz, K., Singer, B.S., Jicha, B.R., 2020. Growth, overprinting, and stabilization of Proterozoic provinces in the southern Lake Superior region. Precambrian Res. 339. https://doi.org/10.1016/j.precamres.2019.105587 Article 105587.
- Jang, B.A., Wang, H.F., 1991. Micromechanical modeling of healed crack orientations as a paleostress indicator: application to Precambrian granite from Illinois to Wisconsin. J. Geophys. Res. 96 (B12), 19,655–19,664. https://doi.org/10.1029/91JB01938.
- Jang, B.A., Wang, H.F., Ren, X., Kowallis, B.J., 1989. Precambrian paleostress from microcracks and fluid inclusions in the Wolf River batholith of central Wisconsin. Geol. Soc. Am. Bull. 101, 1457–1464. https://doi.org/10.1130/0016-7606(1989)101% 3C1457:PPFMAF%3E2.3.CO:2.
- Jones III, J.V., Daniel, C.G., Frei, D., Thrane, K., 2011. Revised regional correlations and tectonic implications of Paleoproterozoic and Mesoproterozoic metasedimentary rocks in northern New Mexico, USA: New findings from detrital zircon studies of the Hondo Group, Vadito Group, and Marqueñas Formation. Geosphere 7, 974–991. https://doi.org/10.1130/GES00614.1.
- Kuiper, K.F., Deino, A., Hilgen, F.J., Krijgsman, W., Renne, P.R., Wijbrans, J.R., 2008. Synchronizing rock clocks of Earth History. Science 320, 500–504. https://doi.org/ 10.1126/science.1154339.
- Ludwig, K.R., 2012. Isoplot 3.75: a geochronological toolkit for Microsoft Excel. Berkeley Geochronology Center Sp. Pub. 5. pp. 1–75.
- Mako, C.A., Williams, M.L., Karlstrom, K.E., Doe, M.F., Powicki, D., Holland, M.E., Gehrels, G., Pecha, M., 2015. Polyphase Proterozoic deformation in the Four Peaks area, central Arizona, and relevance for the Mazatzal orogeny. Geosphere 11, 1975–1995. https://doi.org/10.1130/GES01196.1.
- Malone, D.H., Stein, C.A., Craddock, J.P., Kley, J., Stein, S., Malone, J.E., 2016. Maximum depositional age of the Neoproterozoic Jacobsville sandstone, Michigan: Implications for the evolution of the Midcontinent Rift. Geosphere 12, 1271–1282. https://doi.org/10.1130/GES01302.1.
- Marshak, S., Wilkerson, M.S., DeFrates, J., 2016. Structural geology of the Baraboo District: an introduction. Geol. Soc. Am. Field Guide 43, 13–36. https://doi.org/10.1130/2016.0043(02).

- Marshall, E.W., Lassiter, J.C., Barnes, J.D., Luguet, A., Lissner, M., 2017. Mantle melt production during the 1.4 Ga Laurentian magmatic event: Isotopic constraints from Colorado Plateau mantle xenoliths. Geology 45. https://doi.org/10.1130/G38891.1 519–122.
- McLennan, S.M., Hemming, S.R., Taylor, S.R., Eriksson, K.A., 1995. Early Proterozoic crustal evolution: geochemical and Nd-Pb isotopic evidence from metasedimentary rocks, southwestern North America. Geochim. Cosmochim. Acta 59, 1153–1177. https:// doi.org/10.1016/0016-7037(95)00032-U.
- Medaris Jr., L.G., Singer, B.S., Brown, P.E., Jicha, B.R., Smith, M.E., 2002. Wolf River–age brecciation in the Baraboo Quartzite, Wisconsin: implications for Proterozoic tectonics in the Lake Superior region. Inst. Lake Superior Geol., Program and Abstracts. 48, pp. 24–25. http://www.lakesuperiorgeology.org/.
- Medaris Jr., L.G., Jicha, B.R., Dott Jr., R.H., Singer, B.S., 2009. A 1465 Ma ⁴⁰Ar/³⁹Ar age for the Seeley Slate: implications for metamorphism and deformation in the Baraboo Range, Wisconsin. Inst. Lake Superior Geol., Program and Abstracts. 55, pp. 59–60. http://www.lakesuperiorgeology.org/.
- Medaris Jr., L.G., Dott Jr., R.H., 2001. Sedimentologic, tectonic and metamorphic history of the Baraboo Interval: new evidence from investigations in the Baraboo Range, Wisconsin. Inst. Lake Superior Geol. Field Trip Guidebook 47, 1–21. http://www.lakesuperiorgeology.org/.
- Medaris Jr., L.G., Koellner, S.E., 2010. Ferromagnesian minerals in the Stettin syenite complex, Marathon County, Wisconsin: Compositions and contrasts with the Wolf River Batholith. Inst. Lake Superior Geol., Program and Abstracts 56, 42–43. http://www.lakesuperiorgeology.org/.
- Medaris Jr., L.G., Singer, B.S., 2010. ⁴⁰Ar/³⁹Ar dating of geon 14 K-metasomatism and hydrothermal alteration in the southern Lake Superior region, Geol. Soc. Am. Abstracts with Programs 42 (2), 47. https://gsa.confex.com/gsa/2010NC/webprogram/Paper170715.html.
- Medaris Jr., L.G., Singer, B.S., Dott Jr., R.H., Naymark, A., Johnson, C.M., Schott, R.C., 2003. Late Paleoproterozoic climate, tectonics, and metamorphism in the southern Lake Superior region and proto–North America: evidence from Baraboo Interval quartzites. J. Geol. 111, 243–257. https://doi.org/10.1086/373967.
- Medaris Jr., L.G., Driese, S.G., Stinchcomb, G.E., 2017. The Paleoproterozoic Baraboo paleosol revisited: Quantifying mass fluxes of weathering and metasomatism, chemical climofunctions, and atmospheric pCO₂ in a chemically heterogeneous protolith. Precambrian Res. 301, 179–194. https://doi.org/10.1016/j.precamres.2017.06.010.
- Meijer, A., 2014. The Pinal schist of southern Arizona: a Paleoproterozoic forearc complex with evidence of spreading ridge-trench interaction at ca. 1.65 Ga and a Proterozoic arc obduction event. Geol. Soc. Am. Bull. 126, 1145–1163. https://doi.org/10.1130/ B31002.1.
- Min, K., Mundil, R., Renne, P.R., Ludwig, K.R., 2000. A test for systematic errors in ⁴⁰Ar/³⁹Ar geochronology through comparison with U/Pb analysis of a 1.1 Ga rhyolite. Geochim. Cosmochim. Acta 64, 73–98. https://doi.org/10.1016/S0016-7037(99)00204-5.
- Myers, P.E., Sood, M.K., Berlin, L.A., Falster, A.U., 1984. The Wausau Syenite complex, central Wisconsin. Inst. Lake Superior Geol., Field Trip Guidebook 30, 1–58. http://www.lakesuperiorgeology.org/.
- Nyman, M.W., Karlstrom, K.E., 1997. Pluton emplacement processes and tectonic setting of the 1.42 Ga Signal batholith, SW USA: important role of crustal anisotropy during regional shortening. Precambrian Res. 82, 237–263. https://doi.org/10.1016/S0301-9268(96)00049-6.
- Ojakangas, R.W., Weber, R.E., 1984. Petrography and paleocurrents of the Lower Proterozoic Sioux Quartzite, Minnesota and South Dakota. In: Southwick, D.L. (Ed.), Shorter Contributions to the Geology of the Sioux Quartzite (Early Proterozoic), southwestern Minnesota. Minn. Geol. Sur., Rept. Inv. 32, pp. 1–15 https://doi.org.ezproxy.library. wisc.edu/11299/60753.
- Ojakangas, R.W., Morey, G.B., Southwick, D.L., 2001a. Paleoproterozoic basin development and sedimentation in the Lake Superior region, North America. Sediment. Geol. 141–142, 319–341. https://doi.org/10.1016/S0037-0738(01)00081-1.
- Ojakangas, R.W., Morey, G.B., Green, J.C., 2001b. The mesoproterozoic midcontinent rift system, lake superior region, USA. Sediment. Geol. 141–142, 421–442. https://doi.org/10.1016/S0037-0738(01)00085-9.
- Paton, C., Hellstrom, J., Paul, B., Woodhead, J., Hergt, J., 2011. Iolite: freeware for the visualisation and processing of mass spectrometric data. J. Anal. At. Spectrom. 26, 2508–2518. https://doi.org/10.1039/c1ja10172b.
- Peacock, M.A., 1931. Classification of igneous rock series. J. Geol. 39, 54–67. https://www.istor.org/stable/30064696.
- Pearce, J.A., Harris, N.B.W., Tindle, A.G., 1984. Trace element discrimination diagrams for the tectonic interpretation of granitic rocks. J. Petrol. 25, 956–983. https://doi.org/ 10.1093/petrology/25.4.956.
- Romano, D., Holm, D.K., Foland, K.A., 2000. Determining the extent and nature of Mazatzal–related overprinting of the Penokean orogenic belt in the southern Lake Superior region, north–central USA. Precambrian Res. 104, 25–46. https://doi.org/10.1016/S0301-9268(00)00085-1.
- Rudnick, R.L., Gao, S., 2004. Composition of the continental crust. Treatise Geochem. 3, 1–64. https://doi.org/10.1016/B0-08-043751-6/03016-4.
- Satkowski, A.M., Bickford, M.E., Samson, S.D., Bauer, R.L., Mueller, P.A., Kamenov, G.D., 2013. Geochemical and Hf-Nd isotopic constraints on the crustal evolution of Archean rocks from the Minnesota River Valley, USA. Precambrian Res. 224, 36–50. https://doi.org/10.1016/j.precamres.2012.09.003.
- Schmitz, M.D., Bowring, S.A., Southwick, D.L., Boerboom, T.J., Wirth, K.R., 2006. High-precision U-Pb geochronology in the Minnesota River Valley subprovince and its bearing on the Neoarchean to Paleoproterozoic evolution of the southern Superior Province. Geol. Soc. Am. Bull. 118, 82–93. https://doi.org/10.1130/B25725.1.
- Schneider, D.A., Bickford, M.E., Cannon, W.F., Schulz, K.J., Hamilton, M.A., 2002. Age of volcanic rocks and syndepositional iron formations, Marquette Range Supergroup: implications for the tectonic setting of Paleoproterozoic iron formations of the Lake Superior region. Can. J. Earth Sci. 39, 999–1012. https://doi.org/10.1139/e02-016.

- Schulz, K.J., Cannon, W.F., 2007. The Penokean orogeny in the Lake Superior region. Precambrian Res. 157, 4–25. https://doi.org/10.1016/j.precamres.2007.06.002.
- Schwartz, J.J., Stewart, E.K., Medaris Jr., L.G., 2018. Detrital zircons in the Waterloo Quartzite, Wisconsin: Implications for the ages of deposition and folding of supermature quartzites in the southern Lake Superior region. Inst. Lake Superior Geol., Program and Abstracts 64, 95–96. http://www.lakesuperiorgeology.org/.
- Shand, S.J., 1927. Eruptive Rocks. D. Van Nostrand, New York 360 pp.
- Shaw, C.A., Heizler, M.T., Karlstrom, K.E., 2005. ⁴⁰Ar/³⁹Ar thermochronologic record of 1.45–1.35 Ga intracontinental tectonism in the southern Rocky Mountains: Interplay of conductive and advective heating with intracontinental deformation. In: Karlstrom, K.E., Keller, G.R. (Eds.), The Rocky Mountain Region: an evolving lithosphere. Am. Geophys. Union, Geophys. Mon. 154, pp. 163–181. https://doi.org/10.1029/154GM12.
- Silver, L.T., Bickford, M.E., Van Schmus, W.R., Anderson, J.L., Anderson, T.H., Medaris Jr., L.G., 1977. The 1.4–1.5 b.y. transcontinental anorogenic plutonic perforation of North America. Geol. Soc. Am. Abstracts with Programs 9 (7), 1176–1177.
- Sims, P.K., Van Schmus, W.R., Schulz, K.J., Peterman, Z.E., 1989. Tectono–stratigraphic evolution of the Early Proterozoic Wisconsin magmatic terranes of the Penokean Orogen. Can. J. Earth Sci. 26, 2145–2158. https://doi.org/10.1139/e89-180.
- Sláma, J., et al., 2008. Plesovice zircon A new natural reference material for U–Pb and Hf isotopic analysis. Chem. Geol. 249, 1–35 j.chemgeo.2007.11.005.
- Smith, E.I., 1978. Precambrian rhyolites and granites in south-central Wisconsin: field relations and geochemistry. Geol. Soc. Am. Bull. 89, 875–890. https://doi.org/10.1130/0016-7606(1978)89%3C875:PRAGIS%3E2.0.CO;2.
- Smith, E.I., 1983. Geochemistry and evolution of the early Proterozoic, post–Penokean rhyolites, granites, and related rocks of south-central Wisconsin, U.S.A. In: Medaris, L.G.Jr. (Ed.), Early Proterozoic Geology of the Great Lakes Region. Geol. Soc. Am. Mem. 160, pp. 113–128 https://doi.org/10.1130/mem160-p113.
- Southwick, D.L., Mossler, J.H., 1984. The Sioux quartzite and subjacent regolith in the Cottonwood County basin, Minnesota. In: Southwick, D.L. (Ed.), Shorter Contributions to the Geology of the Sioux Quartzite (Early Proterozoic), southwestern Minnesota. Minn. Geol. Sur., Rept. Inv. 32, pp. 17–44 https://doi.org.ezproxy.library.wisc.edu/11299/60753.
- Southwick, D.L., Morey, G.B., Mossler, J.H., 1986. Fluvial origin of the lower Proterozoic Sioux Quartzite, southwestern Minnesota. Geol. Soc. Am. Bull. 97, 1432–1441. https://doi.org/10.1130/0016-7606(1986)97<1432:FOOTLP>2.0.CO;2.
- Spencer, J.E., Pecha, M.E., Gehrels, G.E., Dickinson, W.R., Domanik, K.J., Quade, J., 2016. Paleoproterozoic orogenesis and quart—arenite deposition in the Little Chino Valley area, Yavapai tectonic province, central Arizona, USA. Geosphere 12, 1–21. https:// doi.org/10.1130/GES01339.1.
- Stacey, J.S., Kramers, J.D., 1975. Approximation of terrestrial lead isotope evolution by a two-stage model. Earth Planet. Sci. Lett. 26, 207–221. https://doi.org/10.1016/0012-821X(75)90088-6.
- Stewart, E.D., Stewart, E.K., Walker, A., Zambito IV, J.J., 2018. Revisiting the Paleoproterozoic Baraboo interval in southern Wisconsin: evidence for syn-depositional tectonism along the south-central margin of Laurentia. Precambrian Res. 314, 221–239. https://doi.org/10.1016/j.precampes.2018.05.010.
- Taylor, S.R., McLennan, S.M., 1985. The Continental Crust: Its Composition and Evolution. Blackwell. Oxford 312 pp.
- Tera, F., Wasserburg, G.J., 1972. U–Th–Pb systematics in three Apollo 14 basalts and the problem of initial Pb in lunar rocks. Earth Planet. Sci. Lett. 14, 281–304. https://doi.org/10.1016/0012-821X(72)90128-8.
- Tucker, R.D., Gower, C.F., 1994. A U–Pb geochronological framework for the Pinware Terrane, Grenville Province, southeast Labrador. J. Geol. 102, 67–78. https://doi.org/10.1086/629648.
- Van Schmus, W.R., Anderson, J.L., 1977. Gneiss and migmatite of Archean age in the Precambrian basement of Central Wisconsin. Geology 5, 45–48. https://doi.org/10.1130/0091-7613(1977)5%3C45:GAMOAA%3E2.0.CO;2.
- Van Schmus, W.R., Medaris Jr., L.G., Banks, P.O., 1975a. Geology and age of the Wolf River Batholith. Wisconsin. Geol. Soc. Am. Bull. 86, 907–914. https://doi.org/10.1130/0016-7606(1975)86%3C907:GAAOTW%3E2.0.CO;2.
- Van Schmus, W.R., Thurman, M.E., Peterman, Z.E., 1975b. Geology and Rb–Sr chronology of Middle Precambrian rocks in eastern and central Wisconsin. Geol. Soc. Am. Bull. 86, 1255–1265. https://doi.org/10.1130/0016-7606(1975)86%3C1255:GARCOM%3E2.0. C0;2.
- Van Schmus, W.R., Schneider, D.A., Holm, D.K., Dodson, S., Nelson, B.K., 2007. New insights into the southern margin of the Archean–Proterozoic boundary in the north-central United States based on U–Pb, Sm–Nd, and Ar–Ar geochronology. Precambrian Res. 157, 80–105. https://doi.org/10.1016/j.precamres.2007.02.011.
- Van Wyck, N., 1995. Oxygen and carbon isotopic constraints on the development of eclogites, Holsnøy, Norway, and major and trace element, common Pb, Sm-Nd, and zircon geochronology constraints on petrogenesis and tectonic setting of pre- and early Proterozoic rocks in Wisconsin. Ph.D.Dissertation, Univ. Wisc.-Madison 292 pp.
- Van Wyck, N., Norman, M., 2004. Detrital zircon ages form Early Proterozoic quartzites, Wisconsin, support rapid weathering and deposition of mature quartz arenites. J. Geol. 112, 305–315. https://doi.org/10.1086/382761.
- Van Wyck, N., Medaris Jr., L.G., Johnson, C.M., 1994. The Wolf River A-type magmatic event in Wisconsin: U/Pb and Sm/Nd constraints on timing and petrogenesis. Inst. Lake Superior Geol. Program and Abstracts 40, 81–82. http://www. lakesuperiorgeology.org/.
- Weiblen, P.W., 1982. Keweenawan intrusive igneous rocks. In: Wold, R.J., Hinze, W.J. (Eds.), Geology and Tectonics of the Lake Superior Basin. Geol. Soc. Am. Mem 156, pp. 57–82. https://doi.org/10.1130/mem156-p57.
- Whitmeyer, S.J., Karlstrom, K.F., 2007. Tectonic model for the Proterozoic growth of North America. Geosphere 3, 220–259. https://doi.org/10.1130/ges00055.1.

- Williams, H.R., 1990. Subprovince accretion tectonics in the southcentral Superior province. Can. J. Earth Sci. 27, 570–581. https://doi.org/10.1139/e90-053.
- Williams, M.L., Karlstrom, K.E., 1996. Looping P-T paths and high-T, low-P middle crustal metamorphism: Proterozoic evolution of the Southwestern United States. Geology 24, 1119–1122. https://doi.org/10.1130/0091-7613(1996)024%3C1119:LPTPAH% 3E2.3.CO:2.
- Williams, M.L., Jercinovic, M.J., Goncalves, P., Mahan, K.H., 2006. Format and philosophy for collecting, compiling, and reporting microprobe monazite ages. Chem. Geol. 225, 1–15. https://doi.org/10.1016/j.chemgeo.2005.07.024.
- Williams, M.L., Jercinovic, M.J., Mahan, K.E., Dumond, G., 2017. Electron microprobe petrochronology. In: Kohn, M.J., Engi, M., Lanari, P. (Eds.), Petrochronology: Methods and Applications. Rev. Mineral. Geochem 83, pp. 153–182.
 Young, G.M., 1983. Tectono-sedimentary history of early Proterozoic rocks of the northern Great Lakes region. In: Medaris Jr., L.G. (Ed.), Early Proterozoic Geology of the Great Lakes Region. Geol. Soc. Am. Mem 160, pp. 15–32. https://doi.org/10.1130/pp. 150-316. mem160-p15.